

## Article

# Comparative Analysis of Accuracy, Simplicity and Generality of Temperature-Based Global Solar Radiation Models: Application to the Solar Map of Asturias

Jesús-Ignacio Prieto <sup>1,\*</sup> , David García <sup>2</sup>  and Ruth Santoro <sup>1</sup>

<sup>1</sup> Department of Physics, University of Oviedo, c/ Federico García Lorca 18, E-33007 Oviedo, Spain; rsantorocastillo@gmail.com

<sup>2</sup> Department of Energy, University of Oviedo, Edificio Departamental Este, c/Wifredo Ricart s/n, E-33204 Gijón, Spain; garciamdavid@uniovi.es

\* Correspondence: jprieto@uniovi.es

**Abstract:** The accuracy, complexity and generality of 13 temperature-based solar radiation models are compared using data measured during 2003–2016 at 21 weather stations in a large coastal area of northern Spain. The comparisons are based on dimensionless statistical indicators calculated for each model at each station, as well as on averages of errors calculated both for the group of eight stations located in the vicinity of the Principality of Asturias and for the set of all stations. Using site-calibrated coefficients, most models provide acceptable estimates, and no model outperforms the rest everywhere. The dispersion of the site-calibrated coefficients is analysed as a function of geographical variables, and general equations are obtained for each model, based on data from the group of eight stations. The results for the remaining stations allow the predictive capability of the models to be assessed in regions where radiometric measurements are not available. In general, models with a larger number of parameters perform worse, while a homogeneous single-parameter model achieves better results. Combined with GIS techniques, this model is used to update the Solar Map of Asturias, whose previous version was based on data from different time periods due to the scarcity of records at the time.

**Keywords:** global solar radiation; temperature-based models; model comparison; general equations; northern Spain; solar map of Asturias



**Citation:** Prieto, J.-I.; García, D.; Santoro, R. Comparative Analysis of Accuracy, Simplicity and Generality of Temperature-Based Global Solar Radiation Models: Application to the Solar Map of Asturias. *Sustainability* **2022**, *14*, 6749. <https://doi.org/10.3390/su14116749>

Academic Editor:  
Luis Hernández-Callejo

Received: 26 April 2022  
Accepted: 24 May 2022  
Published: 31 May 2022

**Publisher's Note:** MDPI stays neutral with regard to jurisdictional claims in published maps and institutional affiliations.



**Copyright:** © 2022 by the authors. Licensee MDPI, Basel, Switzerland. This article is an open access article distributed under the terms and conditions of the Creative Commons Attribution (CC BY) license (<https://creativecommons.org/licenses/by/4.0/>).

## 1. Introduction

Solar energy is one of the main options to meet the growing demand for environmentally friendly energy worldwide. For the development of solar energy programmes, high-quality solar radiation data are needed [1,2], but weather stations with solar radiation records are scattered [3,4]. For this reason, models have been developed for the indirect estimation of global solar radiation (GSR) from abundantly measured weather variables or satellite images.

Most models provide accurate estimates at locations where they can be calibrated, but no model outperforms the others everywhere [5]. For some authors, it is more convenient to select an appropriate one from the literature than developing a new model [6], while others state that the evaluation of most existing models over a wide range of geography and climate is still pending [7].

Comparisons between models require a definition of the objectives and criteria for analysis. The accuracy of the estimates depends on the quality of the measurements [8] and the complexity of the model, i.e. the number and type of influential variables, and the functional relationship. This paper aims to explore the optimal trade-off between accuracy and complexity of existing GSR models, a task proposed in the most exhaustive review carried out so far [6], with the additional objective of, also, assessing complexity

versus generality, i.e., applicability to large geographical areas where GSR measurements are not available. On the other hand, most models are expressed by dimensionally non-homogeneous equations, with coefficients that depend on implicit variables [9]. If the only objective is to improve accuracy by using locally calibrated coefficients, a model with a larger number of variables and adjustment coefficients, i.e., fewer degrees of freedom, may be advantageous, even if it is not dimensionally homogeneous. If, on the contrary, the objective is to compare the ability of a model to be applied to a variety of locations, a simple and homogeneous model is a priori advantageous, by having more degrees of freedom and using ratios between variables.

Among the hundreds of existing GSR models [6,9], a small number of hybrid models include the influence of geographical variables, introducing the possibility of estimating GSR by general equations over regions where radiometric stations are not available for calibration. Most of them are modifications of classical sunshine-based models [10–14], while two other models are based on temperature [15,16], of which only one is dimensionally homogeneous. As air temperature measurement requires low-cost equipment and is widespread [4], temperature-based models have been chosen as the subject of this study.

Thirteen models of low or moderate functional complexity have been selected and compared using data from 21 meteorological stations located in the north of Spain, covering a coastal area of about 1000 km in length. The results of the inter-model comparison serve as the basis to update the Solar Map of Asturias (SMA) [17], an area of about 10,600 km<sup>2</sup> on the Cantabrian coast of Spain, using GIS techniques to represent isolines of monthly GSR averages based on temperature, solar irradiation and topographic variables.

## 2. Materials and Methods

As shown in Figure 1, the inter-model comparison starts with the calibration of each model at each station, i.e., with the calculation of the regression coefficients of the monthly mean data in the period considered. Equations for the site-calibrated coefficients of the eight stations selected as the basis of the SMA are, then, obtained by least-squares fitting, as a function of the ratio between elevation and distance to the sea. The dispersion caused by geographical variables, implicit in the site-calibrated coefficients, is analysed, and the performance of the models is, finally, compared using statistical indicators.

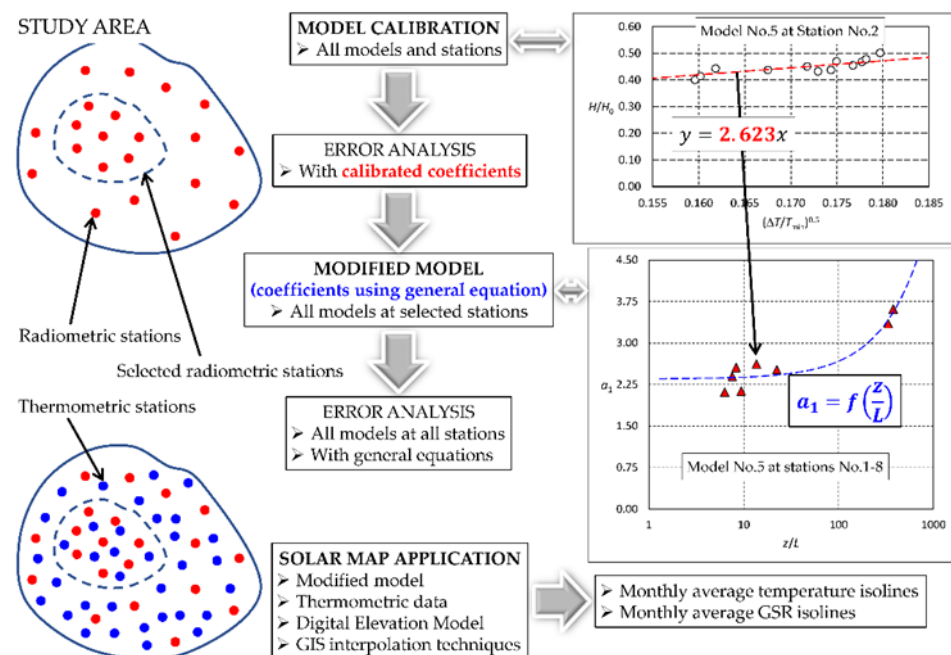


Figure 1. Flowchart of the procedure.

### 2.1. Selection of Temperature-Based GSR Models

There are dozens of GSR models that allow an indirect estimation of the  $H/H_0$  ratio from air temperature measurements [4,6]. The variables used are, usually,  $\Delta T$ ,  $T_m$ ,  $T_{\max}$  and  $T_{\min}$ , and may be related by linear, polynomial, exponential, logarithmic or power functions. The models described below have been selected from models with a maximum of three parameters, seeking a representative variety of the variables used and the types of functional relationship. The models are ordered from the lowest to the highest number of parameters.

#### 2.1.1. Model No.1: Hargreaves and Samani

Hargreaves and Samani suggested that the clearness index could be estimated from the amplitude of the air temperature oscillation [18], by means of the following equation:

$$H/H_0 = a_1 \Delta T^{0.5} \quad (1)$$

The coefficient  $a_1$  was, initially, set at 0.17 for arid and semiarid climates, but, later, values of 0.16 and 0.19 were recommended, respectively, for inland and near the coast [19]. The site dependence of  $a_1$  is, to some extent, due to the fact that Equation (1) is not dimensionally homogeneous [16], as it is impossible to construct a dimensionless group using only the variables  $H$ ,  $H_0$  and  $\Delta T$ . Therefore, this parameter must be interpreted as containing implicit variables.

This pioneering model has been used successfully in numerous localities and has given rise to later variants, some of which will be described below.

#### 2.1.2. Model No.2: Meza and Varas

This model is a variant of the classical Bristow and Campbell approach [20,21], which also uses  $\Delta T$  as a variable, this time included in the exponent of the exponential term of a function with three parameters. The original model, conceived to estimate daily values of the clearness index, was modified by Meza and Varas to analyse monthly averages in Chile using the following equation, involving a single parameter:

$$H/H_0 = 0.75 \left( 1 - e^{-a_1 \Delta T^2} \right) \quad (2)$$

Site-calibrated values of  $a_1$  falling in the range from 0.00150 to 0.01944 were obtained for 20 locations in Chile. As in the previous case, this dispersion is related to implicit variables in  $a_1$ , since Equation (2) is not homogeneous either [9].

#### 2.1.3. Model No.3: Weiss et al.

This model has the same functional form and parameters as the previous model [22], but employs the same variable as the Goodin et al. model [23], i.e.,:

$$H/H_0 = 0.75 \left( 1 - e^{-a_1 \Delta T^2 / H_0} \right) \quad (3)$$

This equation is also not homogeneous, and it is not easy to suggest variables that could be implicit in  $a_1$ , as this coefficient has units of  $J/(m \cdot ^\circ C)^2$ .

#### 2.1.4. Model No.4: Annandale et al.

This model is a modification of model No.1 [15], which has outperformed other temperature-based models in regions of complex orography, such as India [24], due to the incorporation of an altitude correction factor, i.e.,:

$$H/H_0 = a_1 \left( 1 + 2.7 \cdot 10^{-5} z \right) \Delta T^{0.5} \quad (4)$$

The originally recommended value for the parameter is  $a_1 = 0.16$ , but a simple dimensional analysis allows to detect that both  $a_1$  and the factor  $2.7 \cdot 10^{-5}$  contain implicit variables.

#### 2.1.5. Model No.5: Prieto et al.

This model was derived from the dimensional analysis of model No.1 [16]:

$$H/H_0 = a_1(\Delta T/T_{\min})^{0.5} \quad (5)$$

with  $a_1$  being dependent on  $z/L$ , in agreement with the models of Hargreaves and Samani, Allen [25] and Annandale.

#### 2.1.6. Model No.6: Hargreaves et al.

This other evolution of model No.1 [26] has been widely applied under different climatic conditions [27,28] with good results due to the use of two parameters, i.e.:

$$H/H_0 = a_1 + a_2\Delta T^{0.5} \quad (6)$$

#### 2.1.7. Model No.7: Chen et al.

This model was developed from daily GSR data at 48 stations in China [29], obtaining the best results among temperature-based models, such as model No.6. It consists of the following logarithmic equation, which is not homogeneous, so there are implicit variables in at least one of the parameters:

$$H/H_0 = a_1 + a_2 \ln \Delta T \quad (7)$$

#### 2.1.8. Model No.8: Pandey and Katiyar

These authors proposed to express the clearness index as polynomial functions of the ratio between  $T_{\max}$  and  $T_{\min}$ , instead of the difference  $\Delta T$  [30]. Although no mention is made of respect, the procedure yields homogeneous equations. The linear version corresponds to the following equation:

$$H/H_0 = a_1 + a_2(T_{\max}/T_{\min}) \quad (8)$$

#### 2.1.9. Model No.9: Chen and Li

This model was developed for monthly GSR estimates at 13 stations in the Yangtze River Basin in China [31]. It can be considered as the linear and non-homogeneous version of model No.6:

$$H/H_0 = a_1 + a_2\Delta T \quad (9)$$

#### 2.1.10. Model No.10: Present Study

In this new model the exponent 0.5 of model No.5 has been replaced by a fit parameter, resulting in the following homogeneous equation, which can be interpreted as a normalised version of the Richardson model [32]:

$$H/H_0 = a_1(\Delta T/T_{\min})^{a_2} \quad (10)$$

#### 2.1.11. Model No.11: Pandey and Katiyar

This model is the second degree polynomial version of Equation (8) [30]:

$$H/H_0 = a_1 + a_2(T_{\max}/T_{\min}) + a_3(T_{\max}/T_{\min})^2 \quad (11)$$

## 2.1.12. Model No.12: Li et al.

This model was developed for daily GSR estimates and obtained somewhat better results than model No.6, with data measured in Chongqing, China [33]. The same variables as in model No.8 are used, in a non-homogeneous equation with three parameters, i.e.,:

$$H/H_0 = a_1 + a_2 T_{\max} + a_3 T_{\min} \quad (12)$$

## 2.1.13. Model No.13: Hassan et al.

This model obtained the most accurate GSR estimates among 20 temperature-based GSR models evaluated in Egypt at different locations, especially at coastal sites [34], using  $T_m$  as a variable, i.e.,:

$$H/H_0 = a_1 + a_2 H_0 T_m^{a_3} \quad (13)$$

Inclusion of  $H_0$  as a factor implies that  $a_2$  has units of  $m^2/(J \cdot ^\circ C^{a_3})$ , of which the physical interpretation is difficult [9].

## 2.2. Meteorological Stations

Table 1 shows the meteorological stations used for the model analysis. Stations No.1–8 allow comparisons to be made for the same time period at the only radiometric stations in the vicinity of the Principality of Asturias, while stations No.9–21 allow geographical and time period influences to be evaluated. Data from the same station are referred to as stations No.2 and No.13, while the distinction between stations No.17 and No.18 is due not only to the different time period but also to a small change of location. As a whole, the stations cover the whole coastal area of northern Spain, with very different orography and distance to the sea, but similar latitude and not very different climatic characteristics (Figure 2).

**Table 1.** Geographical and climatic characteristic of weather stations.

Station No.	Location	Region	KGCC	$\varphi$	$\lambda$	$z$	$L$	$z/L$	Period
				( $^\circ$ )	( $^\circ$ )	(m)	(km)	(m/km)	
1	Avilés <sup>a</sup>	Asturias	Cfb	43.584	−5.918	12	1.6	7.56	2003–2016
2	Oviedo <sup>b</sup>	“	Cfb	43.354	−5.873	350	25.7	13.61	2003–2016
3	Oviedo <sup>a</sup>	“	Cfb	43.371	−5.836	189	22.8	8.30	2003–2016
4	Mieres <sup>a</sup>	“	Cfb	43.258	−5.773	206	32.8	6.29	2003–2016
5	Langreo <sup>a</sup>	“	Cfb	43.309	−5.706	247	26.3	9.38	2003–2016
6	Gijón <sup>a</sup>	“	Cfb	43.531	−5.672	32	1.4	22.34	2003–2016
7	Niembro <sup>c</sup>	“	Cfb	43.439	−4.850	136	0.4	376.65	2003–2016
8	Santander-CMT <sup>b</sup>	Cantabria	Cfb	43.491	−3.801	60	0.2	333.33	2003–2016
9	A Coruña <sup>b</sup>	Galicia	Csb	43.366	−8.421	60	0.7	85.71	1985–2016
10	Santiago <sup>b</sup>	“	Cfb	42.888	−8.411	372	40.9	9.10	1985–2016
11	A Coruña-Airport <sup>b</sup>	“	Csb	43.304	−8.378	100	4.1	24.59	2004–2016
12	Lugo <sup>b</sup>	“	Csb	43.115	−7.456	446	50.8	8.78	1985–1989
13	Oviedo <sup>b</sup>	Asturias	Cfb	43.354	−5.873	350	25.7	13.61	1975–2016
14	Gijón <sup>d</sup>	“	Cfb	43.545	−5.693	13	0.3	42.85	1993–2005
15	Santander-Centre <sup>b</sup>	Cantabria	Cfb	43.491	−3.819	72	1.1	63.52	1989–1997
16	Bilbao <sup>b</sup>	Basque Country	Cfb	43.298	−2.906	44	9.5	4.63	1985–2016
17	Vitoria (II) <sup>b</sup>	“	Cfb	42.882	−2.735	513	54.2	9.46	2011–2016
18	Vitoria(I) <sup>b</sup>	“	Cfb	42.884	−2.723	508	55.3	9.19	2000–2008
19	San Sebastián <sup>b</sup>	“	Cfb	43.306	−2.041	263	1.1	239.09	1983–2016

Table 1. Cont.

Station No.	Location	Region	KGCC	$\varphi$	$\lambda$	$z$	$L$	$z/L$	Period
				(°)	(°)	(m)	(km)	(m/km)	
20	Pamplona <sup>b</sup>	Navarra	Cfb	42.777	−1.650	461	66.0	6.98	2006–2008
21	Girona <sup>b</sup>	Catalonia	Csa	41.912	+2.763	145	24.7	5.87	2003–2008

<sup>a</sup> Service of Environmental Information of the Principality of Asturias (SIAPA). <sup>b</sup> Spanish State Meteorological Agency (AEMET). <sup>c</sup> Spanish Ministry of Environmental Issues. <sup>d</sup> City Council of Gijón.

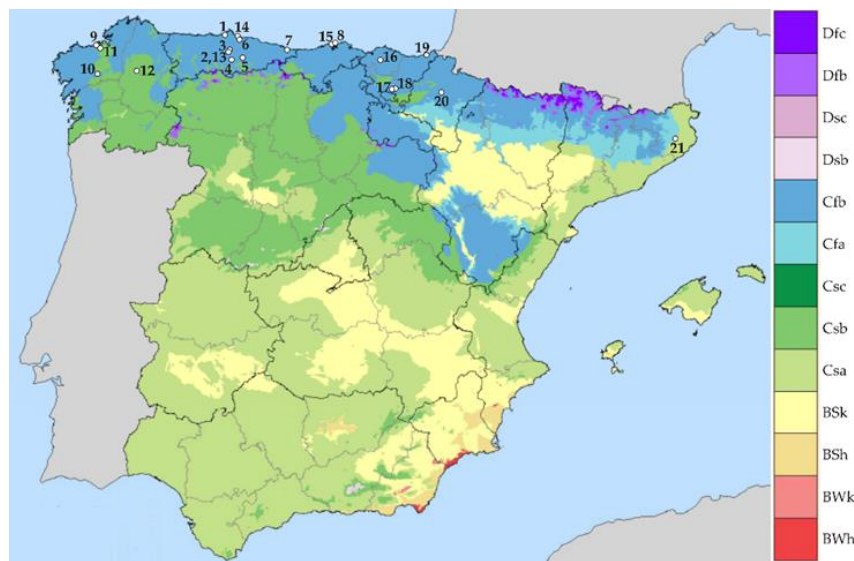


Figure 2. Köppen–Geiger climate classification of meteorological stations [35].

### 2.3. Experimental Data

Tables 2–4 show the average values of maximum and minimum air temperature and solar irradiation for each weather station, during the respective time periods.

Table 2. Average maximum air temperatures at meteorological stations (°C).

No.	Location	Jan	Feb	Mar	Apr	May	Jun	Jul	Aug	Sep	Oct	Nov	Dec	Annual	$\sigma_o$
1	Avilés	13.77	13.44	15.01	16.12	17.88	20.54	22.48	23.08	22.03	19.62	16.57	14.75	17.94	3.35
2	Oviedo	11.90	12.14	14.80	16.43	18.39	21.52	23.22	24.01	22.59	19.56	14.41	12.34	17.61	4.35
3	Oviedo	12.53	12.38	14.56	16.10	18.04	21.08	22.62	23.60	22.24	19.52	14.63	12.68	17.50	4.04
4	Mieres	12.68	13.06	16.00	17.36	19.41	22.74	24.65	25.54	24.10	20.85	15.39	13.05	18.74	4.59
5	Langreo	14.26	13.92	16.35	17.97	20.45	23.70	25.28	26.07	24.55	21.72	16.76	15.32	19.70	4.29
6	Gijón	12.71	12.75	14.30	15.16	17.18	20.09	22.07	22.81	21.57	19.39	15.20	13.34	17.22	3.64
7	Niembro	12.09	11.34	12.73	13.55	15.24	17.92	19.83	20.78	19.55	18.08	14.49	12.81	15.70	3.21
8	Santander-CMT	13.13	12.66	14.51	15.88	17.54	20.44	22.50	23.36	22.06	20.26	16.00	13.86	17.68	3.71
9	A Coruña	13.50	14.08	15.62	16.31	18.44	20.69	22.33	23.00	22.14	19.48	16.00	14.34	17.99	3.32
10	Santiago	11.20	12.25	14.78	16.05	18.54	22.13	24.33	24.68	22.93	18.28	13.97	11.92	17.59	4.75
11	A Coruña-Airport	13.43	13.65	15.64	17.35	19.11	22.05	23.62	23.95	23.32	20.58	16.05	14.33	18.59	3.86
12	Lugo	10.45	11.73	14.65	13.95	18.74	21.14	23.80	24.88	24.48	19.30	13.78	12.08	17.41	5.06
13	Oviedo	11.82	12.68	14.77	15.53	17.99	20.77	22.74	23.27	22.08	18.85	14.47	12.47	17.29	4.03
14	Gijón	14.80	14.80	15.30	16.30	17.90	20.50	22.40	23.50	22.10	19.60	16.10	14.60	18.16	3.17
15	Santander-Centre	13.60	14.50	15.80	15.30	19.20	20.70	23.40	24.10	21.80	19.50	16.40	14.20	18.21	3.56
16	Bilbao	13.69	14.19	16.58	17.80	20.99	23.42	25.45	26.34	24.74	21.73	16.57	14.18	19.64	4.49
17	Vitoria (II)	9.94	8.88	13.66	16.06	19.10	24.08	27.08	27.54	24.67	20.17	13.27	10.15	17.88	6.55
18	Vitoria (I)	9.11	10.59	14.17	15.97	20.07	24.74	25.89	25.96	23.18	18.86	12.18	9.04	17.48	6.24
19	San Sebastián	11.08	11.43	13.38	14.73	17.73	19.98	21.86	22.64	21.21	18.74	14.11	11.91	16.57	4.10
20	Pamplona	10.04	11.12	14.53	18.30	21.24	25.63	28.82	29.54	25.64	20.94	13.88	10.12	19.15	6.90
21	Girona	13.72	14.21	16.93	19.69	23.50	28.54	31.24	30.93	27.07	22.91	17.31	13.99	21.67	6.34

**Table 3.** Average minimum air temperatures at meteorological stations (°C).

No.	Location	Jan	Feb	Mar	Apr	May	Jun	Jul	Aug	Sep	Oct	Nov	Dec	Annual	$\sigma_o$
1	Avilés	7.87	7.15	8.51	10.33	12.28	15.07	17.08	17.20	15.82	12.89	10.28	7.96	11.87	3.56
2	Oviedo	4.82	4.35	5.99	7.66	9.79	12.96	14.73	14.86	13.34	10.86	7.21	5.05	9.30	3.80
3	Oviedo	5.24	4.87	6.41	8.34	10.46	13.62	15.38	15.39	13.72	10.98	7.47	4.86	9.73	3.90
4	Mieres	3.80	3.66	5.63	7.80	10.26	13.82	15.70	15.71	13.80	10.71	6.46	3.58	9.24	4.51
5	Langreo	4.80	4.25	6.01	7.96	10.30	13.65	15.36	15.44	13.64	10.76	7.07	4.42	9.47	4.10
6	Gijón	6.58	6.09	7.62	9.49	11.65	14.87	16.84	17.00	15.41	12.55	9.12	6.73	11.16	3.94
7	Niembro	7.73	6.88	8.23	9.49	11.41	14.39	16.30	16.78	15.69	13.59	10.27	8.44	11.60	3.44
8	Santander-CMT	7.96	7.11	8.58	10.04	12.14	15.15	17.00	17.54	16.10	13.93	10.71	8.59	12.07	3.60
9	A Coruña	8.22	8.13	9.21	10.01	12.17	14.40	16.03	16.47	15.36	13.20	10.52	9.08	11.90	2.98
10	Santiago	4.06	4.17	5.28	6.21	8.41	11.15	12.92	13.14	11.96	9.62	6.59	5.06	8.21	3.29
11	A Coruña-Airport	6.29	4.97	6.59	8.05	10.14	13.08	14.68	14.54	13.04	11.25	8.15	6.14	9.74	3.35
12	Lugo	1.33	1.83	2.63	4.30	6.88	9.40	12.12	10.86	9.78	7.18	4.06	3.26	6.13	3.58
13	Oviedo	4.54	4.73	5.95	6.84	9.39	12.32	14.36	14.69	13.16	10.49	7.15	5.37	9.08	3.66
14	Gijón	8.18	8.16	9.26	10.20	12.80	15.80	17.60	18.30	16.70	13.70	9.81	8.01	12.38	3.77
15	Santander-Centre	7.50	7.70	9.00	9.00	12.50	14.60	17.20	17.80	15.20	12.90	10.50	8.70	11.88	3.52
16	Bilbao	5.28	5.08	6.48	7.86	10.82	13.53	15.55	15.86	13.87	11.61	8.17	6.04	10.01	3.86
17	Vitoria (II)	1.92	0.68	2.60	4.76	6.98	10.32	12.60	12.30	10.47	7.43	4.85	2.32	6.44	4.04
18	Vitoria (I)	1.37	1.29	2.93	4.48	7.26	10.94	11.96	12.38	9.90	8.29	3.85	1.49	6.34	4.10
19	San Sebastián	5.91	5.77	7.26	8.37	11.11	13.86	16.06	16.54	14.81	12.54	8.84	6.84	10.66	3.83
20	Pamplona	1.64	1.72	3.57	6.27	8.77	12.21	14.55	14.73	12.39	9.16	5.57	1.65	7.69	4.78
21	Girona	1.19	1.28	4.08	7.01	10.21	14.73	17.22	17.10	14.29	11.09	5.56	1.80	8.80	5.86

**Table 4.** Average global solar irradiation on horizontal surface at meteorological stations (kWh/(m<sup>2</sup>·day)).

No.	Location	Jan	Feb	Mar	Apr	May	Jun	Jul	Aug	Sep	Oct	Nov	Dec	Annual	$\sigma_o$
1	Avilés	1.146	1.837	2.463	3.269	3.880	4.005	3.907	3.547	2.827	2.015	1.294	1.204	2.616	1.058
2	Oviedo	1.461	2.216	3.343	4.232	4.770	5.012	5.088	4.768	3.991	2.693	1.650	1.433	3.388	1.379
3	Oviedo	1.257	2.046	3.098	4.113	4.672	4.943	4.783	4.586	3.756	2.598	1.624	1.261	3.228	1.369
4	Mieres	1.360	2.038	2.874	3.496	3.937	4.118	4.083	4.025	3.490	2.374	1.477	1.263	2.878	1.081
5	Langreo	1.452	2.083	2.827	3.846	4.098	4.432	4.205	3.951	3.483	2.534	1.659	1.381	2.996	1.098
6	Gijón	1.303	1.869	2.555	3.093	3.441	3.629	3.836	3.748	3.203	2.371	1.513	1.375	2.661	0.918
7	Niembro	1.364	2.122	3.230	4.201	4.878	4.855	4.932	4.605	3.861	2.604	1.543	1.357	3.296	1.381
8	Santander-CMT	1.331	2.186	3.420	4.609	5.452	5.796	5.651	5.170	4.213	2.815	1.599	1.315	3.630	1.667
9	A Coruña	1.404	2.244	3.500	4.565	5.463	6.153	6.213	5.456	4.198	2.642	1.605	1.239	3.723	1.791
10	Santiago	1.293	2.148	3.062	4.020	4.776	5.444	5.383	4.994	4.031	2.569	1.541	1.165	3.369	1.543
11	A Coruña-Airport	1.326	2.227	3.402	4.822	5.464	5.848	6.155	5.453	4.228	2.804	1.621	1.272	3.719	1.762
12	Lugo	1.408	2.069	3.388	3.726	5.067	5.794	5.904	5.421	4.180	2.731	1.797	1.399	3.574	1.633
13	Oviedo	1.490	2.199	3.306	4.143	4.487	4.899	4.825	4.413	3.734	2.572	1.641	1.350	3.255	1.290
14	Gijón	1.639	2.245	3.341	4.131	4.614	4.635	4.636	4.375	3.905	2.566	1.791	1.501	3.282	1.205
15	Santander-Centre	1.431	2.178	3.306	4.085	5.157	5.262	5.352	4.497	3.693	2.455	1.475	1.119	3.334	1.507
16	Bilbao	1.318	2.033	3.094	3.946	4.847	5.141	5.116	4.690	3.691	2.464	1.429	1.173	3.245	1.467

Table 4. Cont.

No.	Location	Jan	Feb	Mar	Apr	May	Jun	Jul	Aug	Sep	Oct	Nov	Dec	Annual	$\sigma_o$
17	Vitoria (II)	1.352	2.190	3.223	4.540	4.933	5.798	5.761	5.106	4.037	2.695	1.310	1.303	3.521	1.660
18	Vitoria (I)	1.428	2.139	3.279	4.162	5.154	5.772	5.952	5.065	4.114	2.632	1.610	1.233	3.545	1.654
19	San Sebastián	1.329	2.063	3.290	4.235	4.896	5.384	5.284	4.632	3.895	2.561	1.516	1.200	3.357	1.510
20	Pamplona	1.473	2.419	3.590	4.400	5.549	5.943	6.768	5.507	4.239	2.963	1.699	1.354	3.825	1.788
21	Girona	1.815	2.712	3.497	4.745	5.664	6.407	6.164	5.139	4.270	2.913	1.980	1.640	3.912	1.648

#### 2.4. Statistical Indicators

The performance of the models has been assessed by comparing the dimensionless statistical indicators considered most representative of the fit between measured and estimated values, namely the relative root mean square error, RRMSE, the relative mean bias error, RMBE, and the coefficient of determination,  $R^2$ . To facilitate comparisons with results from other authors, the Nash–Sutcliffe coefficient of model efficiency, NSE, and the normalised values of the root mean square error and mean bias error, NRMSE and NMBE, respectively, have, also, been calculated, using the mean values of the measurements as references for the latter two. The accuracy of the models is considered high when errors are less than 10% [36], which can only be achieved with high-quality models, as instrumental errors are unavoidable [8]. Depending on the degree of agreement between estimates and measurements,  $R^2$  values range from 0 to 1, while NSE values range from  $-\infty$  to 1.

As an alternative visual tool to the usual scatterplots, Taylor diagrams have been used. Although not yet widely used in GSR-model analysis, this type of chart is recommended for visualising tabulated results [37], since it provides a concise statistical summary of how well patterns match each other in terms of their correlation, their root-mean-square difference, and the ratio of their variances. The Taylor diagram is based on the definition of the centred pattern RMS difference [38]:

$$E' = \sqrt{\frac{1}{n} \sum_{i=1}^n [(s_i - \bar{s}_i)^2 - (o_i - \bar{o}_i)^2]} \quad (14)$$

which is related to the key statistical indicators by means of the following equations:

$$RMSE = (\bar{s}_i - \bar{o}_i)^2 + E'^2 \quad (15)$$

$$(E')^2 = \sigma_o^2 + \sigma_s^2 - 2\sigma_o\sigma_s R \quad (16)$$

The following relationship is derived from normalising Equation (16) by  $\sigma_o$ , and is the basis for the graphical representation of the degree of closeness between a model and the reference data set, using dimensionless variables (Figure 3):

$$E'_n = \sqrt{1 + \sigma_{sn}^2 - 2\sigma_{sn}R} \quad (17)$$

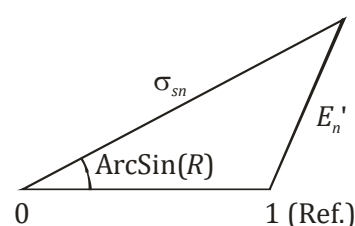


Figure 3. Geometric basis of the Taylor diagram.

### 3. Results and Discussion

#### 3.1. Model Performance with Site-Calibrated Coefficients

Table 5 shows the regression coefficients obtained for each model and station when fitting the experimental monthly GSR data, as well as the corresponding annual average relative errors.

**Table 5.** Site-calibrated coefficients and model performance at meteorological stations.

Station \ Model	No.1	No.2	No.3	No.4	No.5	No.6	No.7	No.8	No.9	No.10	No.11	No.12	No.13	
No.1	$a_1$	0.142	0.017	0.076	0.142	2.397	0.221	0.236	-2.245	0.284	0.603	2248	0.239	0.314
	$a_2$	-	-	-	-	-	0.052	0.063	2.541	0.011	0.141	-4405	0.016	0.017
	$a_3$	-	-	-	-	-	-	-	-	-	-	2158	-0.015	-0.508
	RRMSE (%)	4.85	10.15	40.66	4.85	5.17	4.22	4.23	4.26	4.21	4.27	3.85	3.99	4.92
	RMBE (%)	0.05	-1.68	-22.90	0.04	0.03	0.17	0.17	0.17	0.17	0.17	0.09	0.14	0.16
No.2	$a_1$	0.156	0.013	0.080	0.156	2.623	-0.053	-0.071	-9.460	0.193	3.911	1520	0.177	0.396
	$a_2$	-	-	-	-	-	0.174	0.246	9.627	0.031	0.614	-2964	0.034	0.003
	$a_3$	-	-	-	-	-	-	-	-	-	-	1445	-0.034	0.325
	RRMSE (%)	3.32	7.27	21.65	3.31	3.39	3.29	3.32	3.24	3.26	3.25	3.04	3.22	6.15
	RMBE (%)	0.16	-1.66	-7.01	0.07	0.19	0.11	0.11	0.10	0.10	0.05	0.09	0.10	-0.86
No.3	$a_1$	0.152	0.014	0.070	0.152	2.561	-0.353	-0.375	-11.688	0.037	6.476	3886	0.066	0.334
	$a_2$	-	-	-	-	-	0.279	0.390	11.789	0.050	0.759	-7575	0.040	0.008
	$a_3$	-	-	-	-	-	-	-	-	-	-	3691	-0.036	0.149
	RRMSE (%)	6.89	6.42	34.52	6.88	7.43	6.24	6.25	7.19	6.24	7.17	6.84	4.30	7.67
	RMBE (%)	0.57	-0.04	-14.58	0.50	0.58	0.36	0.36	0.47	0.36	0.24	0.43	0.18	-0.40
No.4	$a_1$	0.126	0.008	0.043	0.126	2.111	-0.372	-0.471	-10.683	0.009	9.244	-1181	0.010	0.353
	$a_2$	-	-	-	-	-	0.246	0.381	10.709	0.040	0.936	2275	0.040	0.236
	$a_3$	-	-	-	-	-	-	-	-	-	-	-1095	-0.040	-1.647
	RRMSE (%)	3.95	3.67	30.40	3.94	3.98	2.96	2.95	3.19	2.96	3.19	3.08	2.94	6.97
	RMBE (%)	0.31	-0.37	-14.58	0.24	0.30	0.09	0.09	0.10	0.09	0.05	0.09	0.09	-2.06
No.5	$a_1$	0.127	0.007	0.038	0.127	2.132	-0.074	-0.146	-8.298	0.163	4.759	2346	0.118	0.400
	$a_2$	-	-	-	-	-	0.150	0.237	8.399	0.024	0.742	-4535	0.030	1388
	$a_3$	-	-	-	-	-	-	-	-	-	-	2191	-0.033	-6.048
	RRMSE (%)	4.65	5.83	29.28	4.65	4.33	4.64	4.66	4.16	4.62	4.16	3.94	3.78	5.30
	RMBE (%)	0.23	-0.29	-16.48	0.16	0.24	0.21	0.21	0.17	0.21	0.09	0.16	0.14	-0.37
No.6	$a_1$	0.149	0.018	0.086	0.149	2.517	-0.238	-0.176	-12.152	0.063	5.754	-1333	-0.082	0.356
	$a_2$	-	-	-	-	-	0.246	0.302	12.257	0.050	0.716	2600	0.067	28390
	$a_3$	-	-	-	-	-	-	-	-	-	-	-1267	-0.063	-7.145
	RRMSE (%)	6.94	8.28	36.50	6.93	7.06	6.22	6.20	6.72	6.24	6.68	6.64	5.15	9.65
	RMBE (%)	0.75	-1.19	-21.39	0.72	0.71	0.39	0.38	0.45	0.39	0.22	0.43	0.28	-0.86
No.7	$a_1$	0.214	0.050	0.221	0.214	3.615	0.580	0.534	6.392	0.509	0.194	-4659	0.233	0.368
	$a_2$	-	-	-	-	-	-0.072	-0.071	-5.873	-0.018	-0.190	9196	0.030	0.004
	$a_3$	-	-	-	-	-	-	-	-	-	-	-4537	-0.023	0.297
	RRMSE (%)	9.21	14.14	42.36	9.20	9.67	7.10	7.10	7.00	7.09	6.99	6.91	5.90	6.54
	RMBE (%)	0.33	-1.61	-22.50	0.21	0.29	0.48	0.48	0.47	0.48	0.24	0.45	0.34	-0.87
No.8	$a_1$	0.198	0.031	0.161	0.198	3.350	-0.564	-0.435	-21.258	-0.039	21.760	-11238	0.010	0.346
	$a_2$	-	-	-	-	-	0.436	0.525	21.308	0.091	0.978	22015	0.063	0.005
	$a_3$	-	-	-	-	-	-	-	-	-	-	-10781	-0.055	0.445
	RRMSE (%)	10.11	8.70	35.00	10.09	10.60	8.76	8.69	9.98	8.82	9.84	9.44	5.84	6.63
	RMBE (%)	1.15	1.04	-12.00	1.06	1.17	0.77	0.76	0.96	0.78	0.48	0.87	0.36	-0.21
No.9	$a_1$	0.193	0.028	0.156	0.193	3.265	-0.876	-0.726	-33.871	-0.210	186.320	-3811	-0.112	0.346
	$a_2$	-	-	-	-	-	0.548	0.666	33.628	0.113	1.553	7433	0.083	0.003
	$a_3$	-	-	-	-	-	-	-	-	-	-	-3624	-0.076	0.658
	RRMSE (%)	9.46	5.35	30.53	9.45	9.89	4.67	4.66	5.46	4.68	5.47	5.40	3.76	4.38
	RMBE (%)	1.44	1.32	-6.15	1.39	1.46	0.23	0.22	0.32	0.23	0.15	0.29	0.15	-0.22
No.10	$a_1$	0.142	0.009	0.068	0.142	2.381	-0.096	-0.145	-8.324	0.164	3.948	-130	0.195	0.328
	$a_2$	-	-	-	-	-	0.173	0.260	8.474	0.029	0.650	244	0.022	0.002
	$a_3$	-	-	-	-	-	-	-	-	-	-	-114	-0.018	0.732
	RRMSE (%)	4.59	14.04	17.26	4.58	4.98	3.94	3.87	4.20	4.03	4.14	4.13	3.72	6.56
	RMBE (%)	0.57	-6.43	0.85	0.48	0.65	0.16	0.16	0.19	0.17	0.09	0.18	0.16	-0.04

Table 5. Cont.

Station \ Model	No.1	No.2	No.3	No.4	No.5	No.6	No.7	No.8	No.9	No.10	No.11	No.12	No.13	
No.11	$a_1$	0.161	0.013	0.073	0.161	2.701	-0.693	-0.780	-19.355	-0.115	46.338	-1138	-0.016	0.335
	$a_2$	-	-	-	-	-	0.393	0.577	19.230	0.067	1.322	2190	0.047	0.005
	$a_3$	-	-	-	-	-	-	-	-	-	-	-1053	-0.039	0.465
	RRMSE (%)	9.76	6.01	31.15	9.75	10.25	5.93	5.92	6.92	5.98	6.91	6.91	4.26	6.48
	RMBE (%)	1.47	0.86	-7.46	1.43	1.50	0.38	0.36	0.52	0.39	0.24	0.46	0.21	-0.15
No.12	$a_1$	0.139	0.007	0.047	0.138	2.317	-0.098	-0.218	-6.969	0.185	3.587	-182	0.268	0.376
	$a_2$	-	-	-	-	-	0.168	0.283	7.144	0.025	0.637	342	0.013	0.001
	$a_3$	-	-	-	-	-	-	-	-	-	-	-161	-0.005	1.212
	RRMSE (%)	5.67	11.37	22.50	5.66	6.14	5.28	5.26	5.72	5.34	5.66	5.64	3.67	7.21
	RMBE (%)	0.59	-5.22	-5.30	0.47	0.66	0.29	0.28	0.34	0.30	0.16	0.32	0.14	0.18
No.13	$a_1$	0.151	0.013	0.076	0.151	2.545	0.061	0.050	-7.036	0.243	2.274	1444	0.224	0.403
	$a_2$	-	-	-	-	-	0.130	0.183	7.258	0.023	0.468	-2815	0.027	0.004
	$a_3$	-	-	-	-	-	-	-	-	-	-	1372	-0.028	-0.060
	RRMSE (%)	3.27	7.42	22.27	3.27	3.15	3.20	3.22	3.12	3.19	3.13	2.96	3.11	4.72
	RMBE (%)	0.06	-1.35	-7.92	-0.03	0.08	0.10	0.10	0.09	0.10	0.05	0.08	0.09	-1.00
No.14	$a_1$	0.186	0.026	0.108	0.185	3.131	0.197	0.227	-5.017	0.323	1.221	-2551	0.107	0.433
	$a_2$	-	-	-	-	-	0.104	0.125	5.355	0.021	0.258	4997	0.047	717
	$a_3$	-	-	-	-	-	-	-	-	-	-	-2447	-0.042	-4.943
	RRMSE (%)	4.83	12.70	42.49	4.83	5.28	4.19	4.14	4.34	4.25	4.24	3.41	3.79	5.32
	RMBE (%)	-0.06	-3.94	-27.50	-0.09	-0.14	0.19	0.18	0.20	0.19	0.09	0.12	0.15	-0.27
No.15	$a_1$	0.172	0.022	0.114	0.172	2.911	-0.532	-0.454	-17.917	-0.050	19.865	-8581	-0.100	0.326
	$a_2$	-	-	-	-	-	0.384	0.481	17.952	0.076	1.005	16773	0.073	0.019
	$a_3$	-	-	-	-	-	-	-	-	-	-	-8197	-0.067	-0.106
	RRMSE (%)	7.79	6.07	33.84	7.78	8.21	6.12	6.06	7.36	6.20	7.27	6.23	3.96	5.34
	RMBE (%)	0.80	0.32	-11.77	0.76	0.80	0.40	0.39	0.55	0.41	0.27	0.38	0.17	-0.56
No.16	$a_1$	0.136	0.009	0.052	0.136	2.285	-0.413	-0.508	-13.354	-0.002	16.777	-726	0.048	0.335
	$a_2$	-	-	-	-	-	0.269	0.411	13.322	0.044	1.090	1393	0.036	0.003
	$a_3$	-	-	-	-	-	-	-	-	-	-	-668	-0.034	0.489
	RRMSE (%)	5.44	3.83	27.68	5.43	6.00	2.44	2.43	3.22	2.47	3.22	3.13	2.01	4.83
	RMBE (%)	0.69	-0.89	-6.52	0.66	0.73	0.06	0.06	0.11	0.07	0.05	0.10	0.04	-0.35
No.17	$a_1$	0.133	0.006	0.048	0.133	2.234	0.001	-0.079	-5.766	0.219	2.559	-90	0.118	0.303
	$a_2$	-	-	-	-	-	0.133	0.219	5.970	0.020	0.543	168	0.035	0.016
	$a_3$	-	-	-	-	-	-	-	-	-	-	-78	-0.045	0.039
	RRMSE (%)	7.25	20.97	17.85	7.24	7.23	7.26	7.25	7.11	7.31	7.01	7.04	5.49	8.34
	RMBE (%)	0.48	-11.14	-1.51	0.38	0.63	0.49	0.48	0.48	0.50	0.23	0.46	0.31	-1.41
No.18	$a_1$	0.137	0.007	0.054	0.136	2.287	-0.007	-0.080	-6.118	0.215	2.541	42	0.244	0.354
	$a_2$	-	-	-	-	-	0.139	0.224	6.320	0.021	0.533	-86	0.017	0.003
	$a_3$	-	-	-	-	-	-	-	-	-	-	44	-0.015	0.542
	RRMSE (%)	2.23	18.41	11.55	2.23	2.57	2.23	2.36	2.41	2.18	2.47	2.40	1.92	4.62
	RMBE (%)	0.08	-9.25	1.36	-0.02	0.21	0.04	0.05	0.05	0.05	0.03	0.06	0.04	0.10
No.19	$a_1$	0.179	0.025	0.145	0.179	3.021	-0.431	-0.328	-20.886	-0.001	25.056	-7191	0.054	0.336
	$a_2$	-	-	-	-	-	0.357	0.430	20.886	0.074	1.047	14073	0.057	0.006
	$a_3$	-	-	-	-	-	-	-	-	-	-	-6884	-0.053	0.306
	RRMSE (%)	6.51	4.79	28.58	6.49	7.05	4.35	4.26	5.36	4.45	5.33	4.10	3.21	5.55
	RMBE (%)	0.76	-0.51	-6.95	0.63	0.79	0.21	0.20	0.31	0.22	0.14	0.16	0.11	-0.12
No.20	$a_1$	0.145	0.007	0.057	0.145	2.435	-0.054	-0.156	-7.172	0.211	3.367	-30	0.218	0.378
	$a_2$	-	-	-	-	-	0.161	0.266	7.360	0.024	0.602	51	0.023	0.003
	$a_3$	-	-	-	-	-	-	-	-	-	-	-21	-0.023	0.575
	RRMSE (%)	4.55	14.86	15.36	4.53	4.86	4.36	4.34	4.45	4.42	4.42	4.43	4.42	6.35
	RMBE (%)	0.44	-7.14	0.85	0.33	0.58	0.19	0.19	0.20	0.20	0.10	0.20	0.20	-0.33
No.21	$a_1$	0.140	0.007	0.039	0.140	2.357	-0.295	-0.513	-8.370	0.104	4.969	2759	0.221	0.453
	$a_2$	-	-	-	-	-	0.222	0.398	8.486	0.031	0.742	-5287	0.021	0.002
	$a_3$	-	-	-	-	-	-	-	-	-	-	2534	-0.018	0.386
	RRMSE (%)	3.82	3.89	24.65	3.81	4.58	3.46	3.48	4.43	3.45	4.43	3.85	2.83	2.80
	RMBE (%)	0.24	-0.18	-10.15	0.19	0.26	0.12	0.12	0.19	0.12	0.10	0.15	0.08	-0.47

In general, all models perform well at all stations, except model No.3, with noticeably high relative errors, and, to a lesser extent, model No.2, which shows RRMSE values somewhat higher than 10% at stations No.1, No.7, No.10, No.12, No.14 and No.20, and in the order of 20% at stations No.17 and No.18.

In each of the stations, it is observed that the lowest RRMSE values are obtained using models with a greater number of coefficients. However, model No.13 generally presents less favourable results than models No.11 and No.12, as well as other models with fewer coefficients, except at stations No.7, No.8, No.9, No.11 and No.15, which are very close to the coastline, and at station No.21.

On the other hand, the annual average RMBE values indicate that models No.2, No.3 and, to a lesser extent, No.13, tend to underestimate solar irradiation in most stations.

Table 6 shows for each model the averages of the statistical indicators obtained for the set of eight stations with the same time period, as well as for the set of 21 stations. Normalised values can be converted to ordinary variables, taking into account that the average of the 96 monthly GSR data for the eight stations is  $\bar{H} = 3.087\text{kWh}/(\text{m}^2\cdot\text{day})$ , with a standard deviation  $\sigma_o = 1.309\text{ kWh}/(\text{m}^2\cdot\text{day})$  caused by the natural variability of irradiation, while the average of the 252 monthly GSR data for the 21 stations is  $\bar{H} = 3.350\text{ kWh}/(\text{m}^2\cdot\text{day})$ , with standard deviation  $\sigma_o = 1.509\text{ kWh}/(\text{m}^2\cdot\text{day})$ . Since the signs of RMBE and NMBE may not coincide, it should be noted that interpretations based on the sum of relative values are more correct. As can be seen, most of statistical indicators for all models improve when analysing data for the set of 21 stations and, for both sets of stations, all models, except model No.3, provide high-quality estimates.

Table 6. Summary of model performance with site-calibrated coefficients.

Station \ Model	No.1	No.2	No.3	No.4	No.5	No.6	No.7	No.8	No.9	No.10	No.11	No.12	No.13	
Stations No.1–8	RRMSE (%)	6.66	8.58	34.36	6.65	6.93	5.74	5.73	6.14	5.75	6.10	5.88	4.52	6.87
	NRMSE (%)	6.30	9.31	44.22	6.33	6.59	5.84	5.84	6.09	5.83	6.26	5.92	4.28	7.71
	RMBE (%)	0.44	−0.72	−16.43	0.38	0.44	0.32	0.32	0.36	0.32	0.18	0.33	0.21	−0.82
	NMBE (%)	−0.74	−2.12	−27.78	−0.81	−0.96	−0.48	−0.48	−0.66	−0.49	−0.84	−0.70	−0.10	0.20
	NSE	0.9779	0.9517	−0.0879	0.9777	0.9758	0.9811	0.9810	0.9794	0.9811	0.9782	0.9805	0.9898	0.9670
	R <sup>2</sup>	0.9799	0.9568	0.3873	0.9799	0.9790	0.9819	0.9819	0.9809	0.9819	0.9800	0.9822	0.9898	0.9763
	$\sigma_{sn}$	0.9488	0.9275	0.4082	0.9479	0.9376	0.9642	0.9644	0.9544	0.9640	0.9521	0.9535	0.9919	1.0844
	$E'_n$ (%)	14.76	21.39	81.15	14.80	15.38	13.72	13.73	14.28	13.71	14.63	13.86	10.09	18.17
All stations	RRMSE (%)	6.37	10.43	29.66	6.36	6.70	5.09	5.07	5.55	5.11	5.51	5.25	4.01	6.19
	NRMSE (%)	6.00	8.94	36.53	6.02	6.39	5.41	5.38	5.94	5.45	6.05	5.41	4.03	6.86
	RMBE (%)	0.53	−2.35	−10.46	0.46	0.56	0.26	0.26	0.31	0.26	0.15	0.27	0.17	−0.53
	NMBE (%)	−0.95	−1.94	−20.51	−1.02	−1.15	−0.46	−0.45	−0.65	−0.47	−0.78	−0.56	−0.14	0.33
	NSE	0.9823	0.9606	0.3420	0.9821	0.9799	0.9856	0.9857	0.9826	0.9854	0.9819	0.9856	0.9920	0.9768
	R <sup>2</sup>	0.9852	0.9632	0.5764	0.9853	0.9842	0.9862	0.9864	0.9839	0.9860	0.9833	0.9866	0.9920	0.9826
	$\sigma_{sn}$	0.9422	1.0086	0.5952	0.9414	0.9313	0.9699	0.9699	0.9597	0.9697	0.9585	0.9639	0.9906	1.0672
	$E'_n$ (%)	13.15	19.38	67.12	13.17	13.95	11.97	11.91	13.11	12.05	13.33	11.95	8.94	15.22

Figure 4a,b show the scatterplots of monthly GSR estimates versus measurements, obtained, respectively, for model No.2, which would be the least satisfactory, if model No.3 is discarded, and for the best performing model, i.e., model No.12.

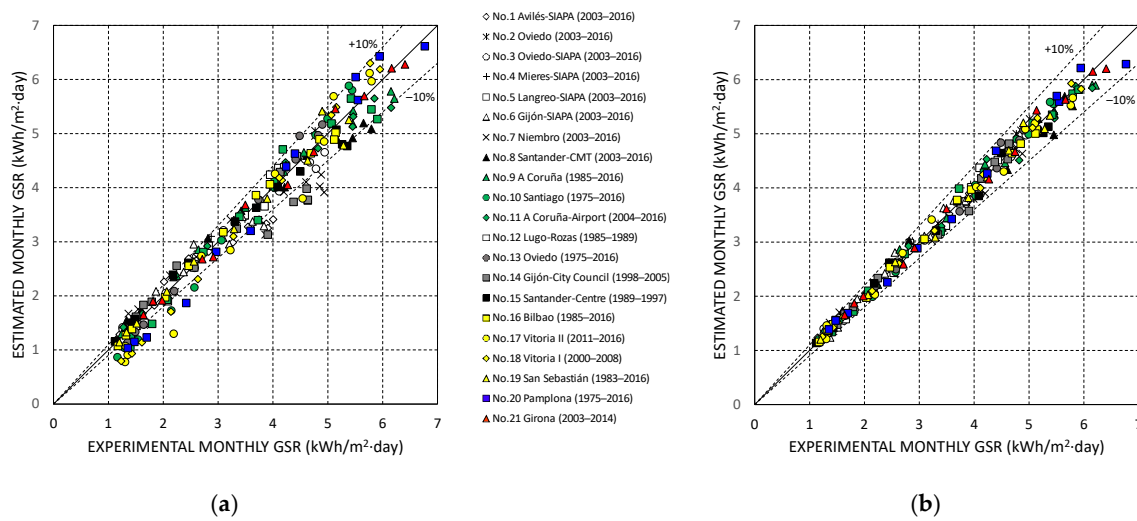


Figure 4. Comparison between monthly GSR data and estimates using site-calibrated coefficients: (a) model No.2 and (b) model No.12.

Figure 5a shows the Taylor diagram obtained for the performance of the models at the eight stations having the same time period, while Figure 5b represents the diagram for the set of 21 stations. In short, the plots, clearly, corroborate the observations previously derived from the tabulated results, with generally acceptable accuracy and no major influence of the time period on the performance of the models.

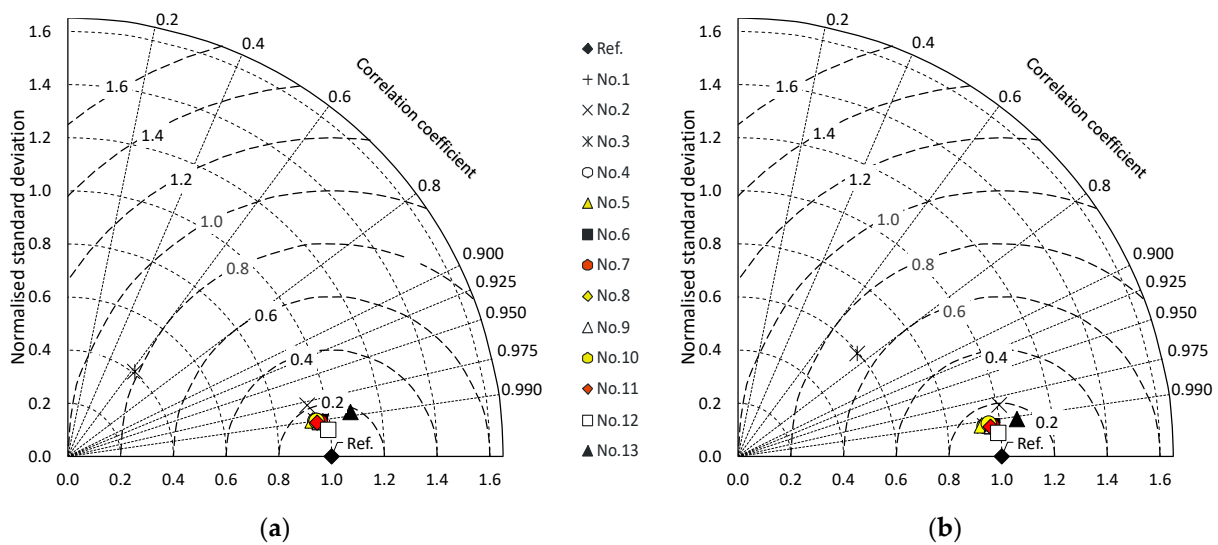


Figure 5. Comparison of model performance with site-calibrated coefficients: (a) Stations No.1–8 and (b) all stations.

### 3.2. Model Performance with Coefficients Obtained from General Equations

Equations (18)–(42) are the result of the geographical dispersion analysis of the site-calibrated coefficients obtained for each model at stations No.1–8. The trend lines with the best NSE values are shown in Figures 6–8, where the site-calibrated coefficients for stations No.9–21 are, also, plotted to facilitate comparisons.

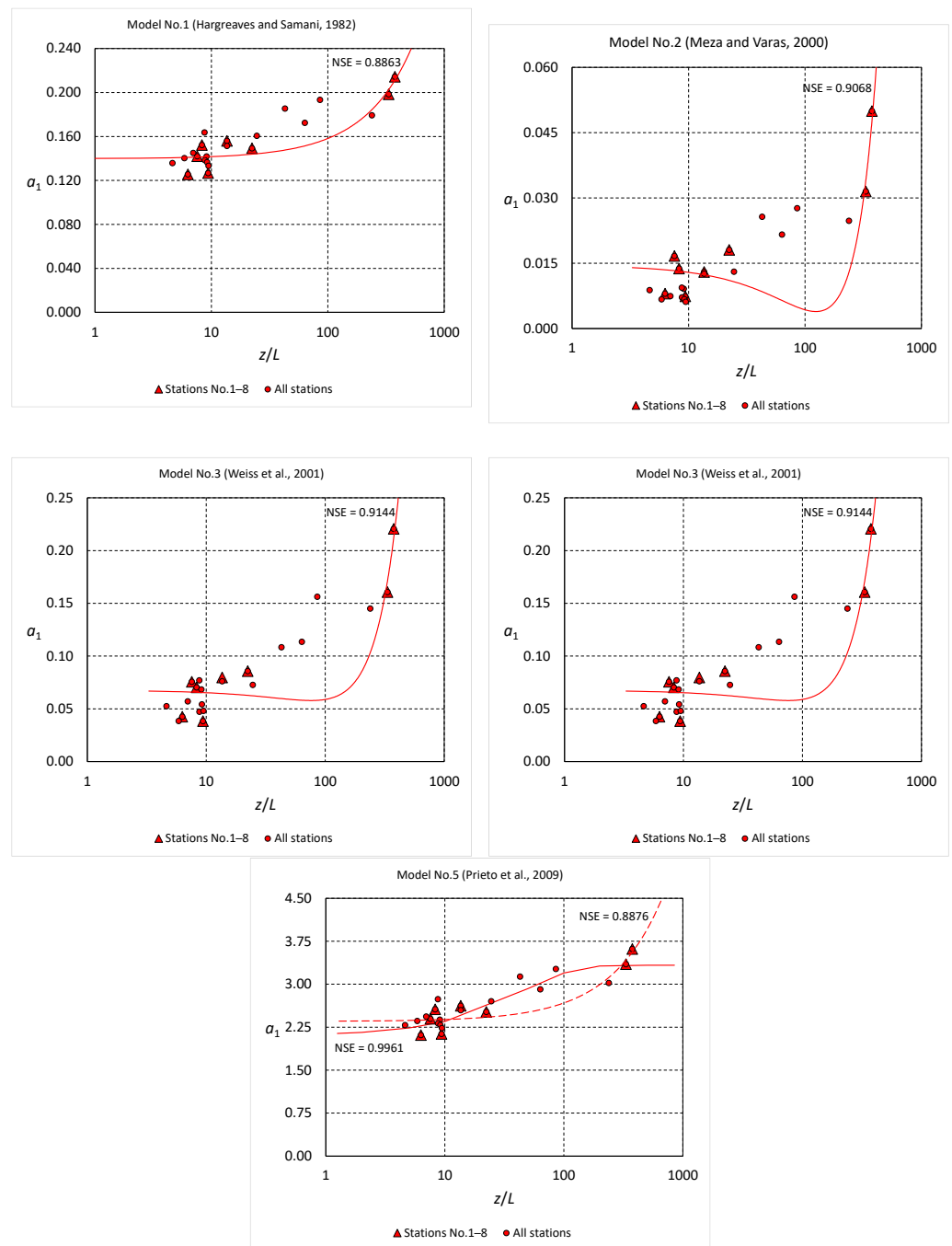


Figure 6. Dispersion of regression parameters for one-parameter models.

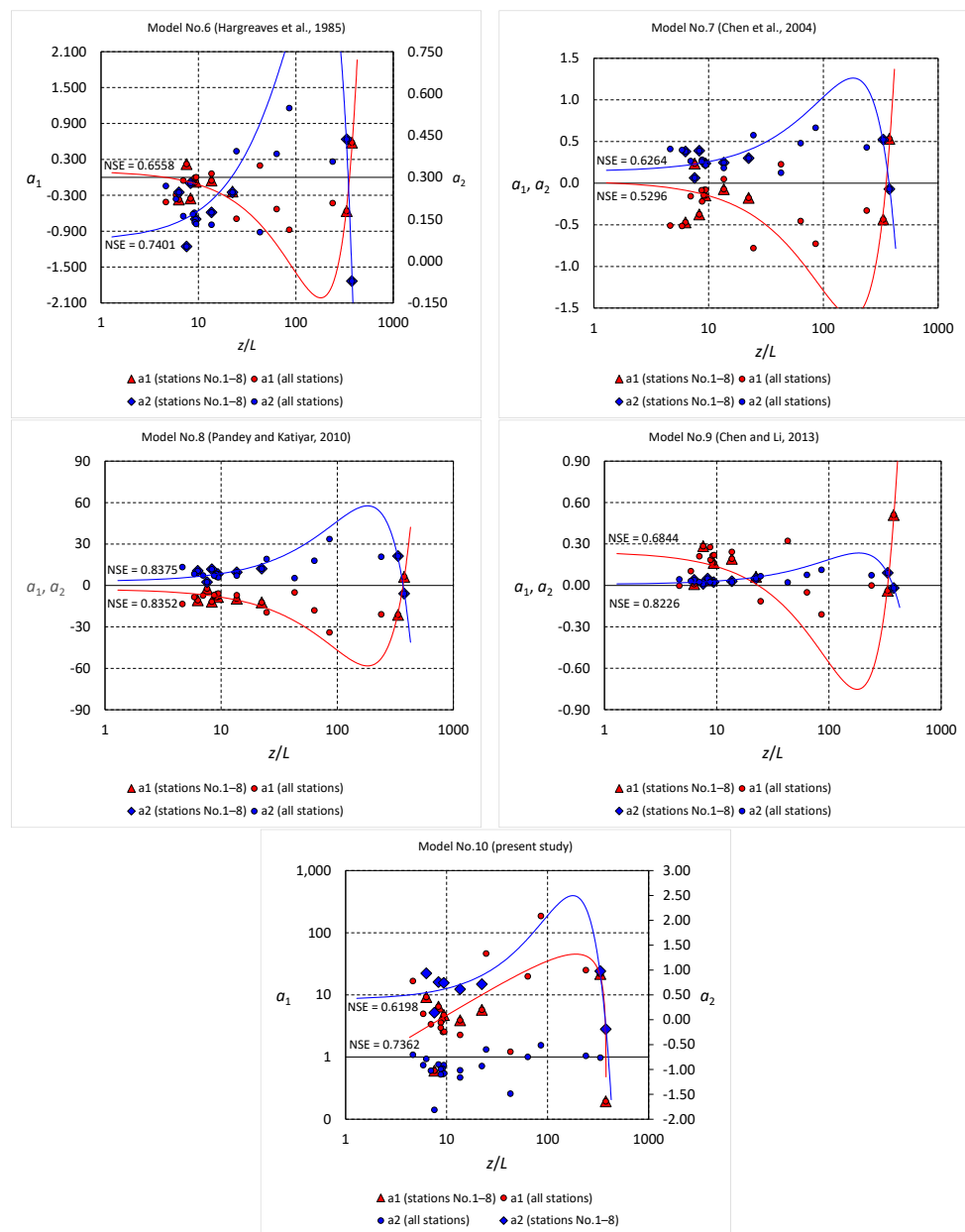


Figure 7. Dispersion of regression parameters for two-parameter models.

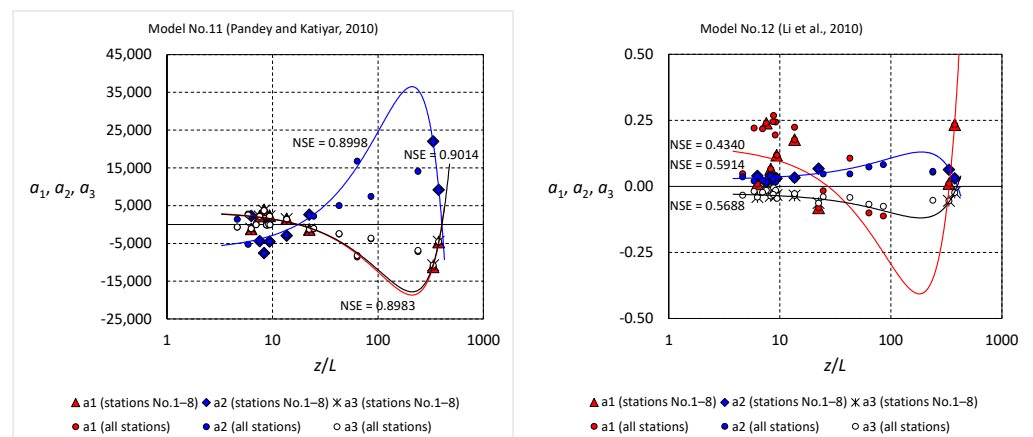
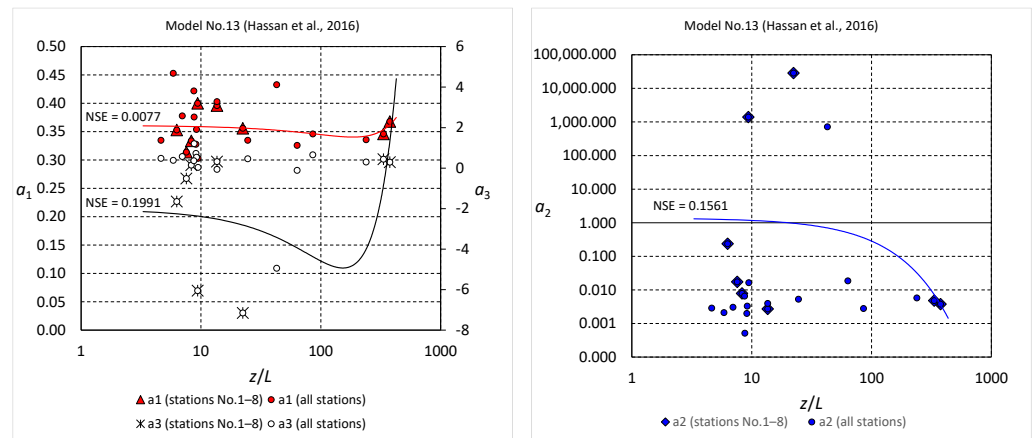


Figure 8. Cont.



**Figure 8.** Dispersion of regression parameters for three-parameter models.

The variable used was the  $z/L$  ratio because longitude is not an influential variable, variations in latitude are small and the use of  $z$  and  $L$  as independent variables would lead to non-homogeneous equations. In the search for models of maximum simplicity, polynomial trend lines with a degree greater than two have not been considered. However, for model No.5, an equation of the type introduced in a previous paper [9], with an exponential term and three regression coefficients, has, also, been obtained for comparison.

Model No.1:

$$a_1 = 0.139833 + 0.000181z/L + 2.11 \cdot 10^{-8}(z/L)^2 \quad (18)$$

Model No.2:

$$a_1 = 0.014543 - 0.000171z/L + 6.91 \cdot 10^{-7}(z/L)^2 \quad (19)$$

Model No.3:

$$a_1 = 0.067672 - 0.000259z/L + 1.71 \cdot 10^{-6}(z/L)^2 \quad (20)$$

Model No.4:

$$a_1 = 0.139742 + 0.000183z/L + 1.68 \cdot 10^{-8}(z/L)^2 \quad (21)$$

Model No.5:

$$a_1 = 2.351488 + 0.003207z/L + 6.51 \cdot 10^{-9}(z/L)^2 \quad (22)$$

$$a_1 = 3.332 - 1.225e^{-0.022z/L} \quad (23)$$

Model No.6:

$$a_1 = 0.106637 - 0.023557z/L + 0.000065(z/L)^2 \quad (24)$$

$$a_2 = 0.072081 + 0.011131z/L - 0.000030(z/L)^2 \quad (25)$$

Model No.7:

$$a_1 = 0.027675 - 0.018355z/L + 0.000052(z/L)^2 \quad (26)$$

$$a_2 = 0.137861 + 0.012377z/L - 0.000034(z/L)^2 \quad (27)$$

Model No.8:

$$a_1 = -2.522739 - 0.611678z/L + 0.001679(z/L)^2 \quad (28)$$

$$a_2 = 2.752747 + 0.602542z/L - 0.001653(z/L)^2 \quad (29)$$

Model No.9:

$$a_1 = 0.244437 - 0.011180z/L + 0.000031(z/L)^2 \quad (30)$$

$$a_2 = 0.00766 + 0.002467z/L - 0.000007(z/L)^2 \quad (31)$$

Model No.10:

$$a_1 = 0.054766 + 0.475066z/L - 0.001249(z/L)^2 \quad (32)$$

$$a_2 = 0.270027 + 0.261392 \ln a_1 \quad (33)$$

Model No.11:

$$a_1 = 3540.407793 - 211.316172z/L + 0.502365(z/L)^2 \quad (34)$$

$$a_2 = -6909.900957 + 412.544347z/L - 0.980072(z/L)^2 \quad (35)$$

$$a_3 = 3371.847460 - 201.339882z/L + 0.477983(z/L)^2 \quad (36)$$

Model No.12:

$$a_1 = 0.156048 - 0.006212z/L + 0.000017(z/L)^2 \quad (37)$$

$$a_2 = 0.025634 + 0.001109z/L - 0.000003(z/L)^2 \quad (38)$$

$$a_3 = -0.025711 - 0.001009z/L + 0.000003(z/L)^2 \quad (39)$$

Model No.13:

$$a_1 = 0.360945 - 0.000221z/L + 0.000001(z/L)^2 \quad (40)$$

$$a_2 = 0.007763 e^{-2.064736a_3} \quad (41)$$

$$a_3 = -2.020620 - 0.038092z/L + 0.000125(z/L)^2 \quad (42)$$

In the group of one-parameter models, the NSE values are relatively high and similar if trend lines based on second-degree polynomials are used. However, as can be seen in Figure 6, the NSE value obtained for model No.5, using the exponential Equation (23), significantly outperforms the value corresponding to the polynomial Equation (22), represented by a dashed line. Note that Equation (23) provides asymptotes for  $a_1$  at extreme values of the  $z/L$  range, which is consistent with the influence of the distance to the sea assumed in model No.1 [9,16].

The dispersion is greater in the groups of models with two or three parameters, with models No.8 and No.11 being the only ones that reach NSE values relatively close to those obtained with one-parameter models.

As Figure 9 shows, there is a high degree of correlation between coefficients of some models. After performing an error analysis, it was found that Equations (33) and (41) resulted in more accurate irradiation estimates than the alternative polynomial equations as a function of  $z/L$ .

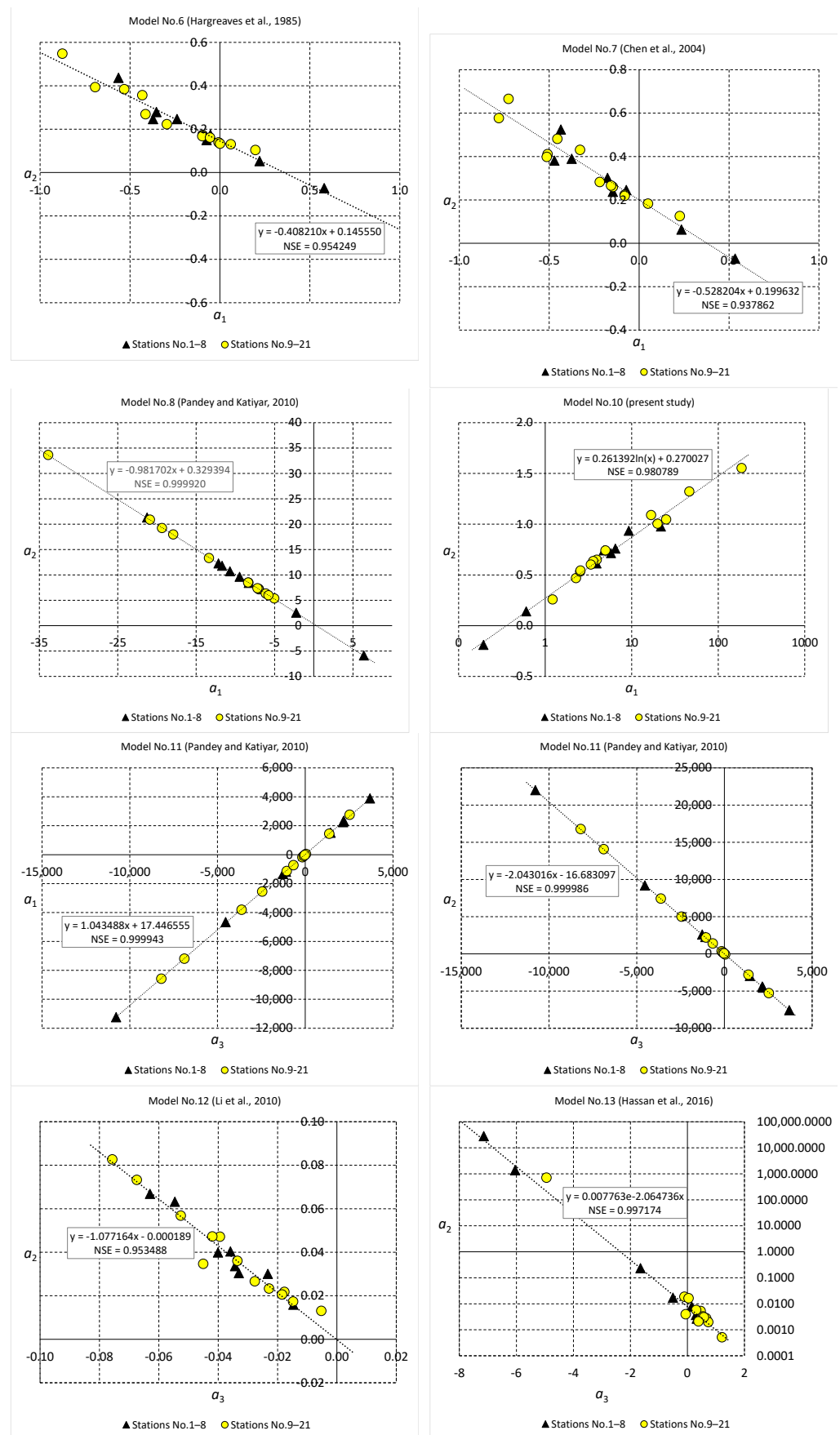


Figure 9. Correlation between regression parameters.

Tables 7 and 8 show, respectively, the annual mean relative errors obtained with general equations for each model at each station, and the averages of statistical indicators for stations No.1–8 and for the 21 stations as a whole.

**Table 7.** Model performance with general equations at meteorological stations.

Station \ Model	No.1	No.2	No.3	No.4	No.5	No.6	No.7	No.8	No.9	No.10	No.11	No.12	No.13
No.1 RRMSE (%)	4.85	19.27	43.72	4.86	6.52	11.58	13.78	10.60	9.75	5.70	17.38	8.81	8.31
No.1 RMBE (%)	−0.55	−17.04	−30.62	−0.59	−4.25	−10.57	−12.74	−9.56	−8.71	0.33	14.98	−7.49	6.80
No.2 RRMSE (%)	9.16	8.56	27.07	9.15	8.04	6.29	7.06	6.50	5.52	3.51	4.18	7.77	17.09
No.2 RMBE (%)	−8.65	−4.82	−19.09	−8.61	−7.41	−5.21	−6.16	−5.67	−4.17	−0.85	−1.59	−6.51	−15.99
No.3 RRMSE (%)	9.22	6.92	35.65	9.30	11.38	14.03	14.25	14.70	13.87	7.49	8.90	10.94	13.39
No.3 RMBE (%)	−6.66	−2.92	−18.47	−6.65	−9.21	−12.81	−13.08	−13.28	−12.60	−2.54	−6.04	−9.57	−10.39
No.4 RRMSE (%)	13.30	36.47	32.05	13.31	8.74	4.51	4.76	4.10	4.22	17.91	40.73	12.28	6.76
No.4 RMBE (%)	12.55	36.25	13.03	12.56	7.63	2.37	2.74	1.43	1.84	17.35	38.61	11.69	−1.85
No.5 RRMSE (%)	12.96	38.08	29.34	12.97	10.88	11.71	10.86	11.10	12.68	23.28	46.67	18.01	9.18
No.5 RMBE (%)	11.87	37.45	15.68	11.89	9.80	10.54	9.59	10.11	11.58	22.70	45.32	16.96	−7.45
No.6 RRMSE (%)	7.27	32.54	45.49	7.29	7.94	6.50	7.04	6.98	6.56	8.00	35.92	7.58	10.69
No.6 RMBE (%)	−2.94	−31.87	−37.79	−2.96	3.33	−0.46	−2.37	0.40	1.24	−4.57	34.13	−5.52	1.69
No.7 RRMSE (%)	9.14	14.46	42.98	9.15	11.69	7.71	8.39	7.17	7.33	31.61	7.08	5.86	20.71
No.7 RMBE (%)	−1.19	−4.18	−24.42	−1.19	−7.57	−3.59	−4.98	−2.25	−2.54	−30.98	−1.64	−0.54	13.25
No.8 RRMSE (%)	10.77	10.76	34.58	10.74	10.50	9.68	10.03	10.53	9.45	32.00	9.38	6.71	18.78
No.8 RMBE (%)	3.29	5.78	−8.57	3.29	0.59	3.38	4.18	2.69	2.70	−31.29	−1.03	3.11	−16.81
No.9 RRMSE (%)	19.91	73.61	57.01	19.89	9.69	16.55	16.01	15.47	17.28	26.80	65.36	9.71	26.99
No.9 RMBE (%)	−18.43	−73.60	−54.25	−18.41	−2.23	15.11	14.63	14.10	15.77	−26.42	64.42	−8.66	−25.03
No.10 RRMSE (%)	4.56	18.87	16.99	4.74	5.07	4.79	5.24	5.01	4.47	9.42	31.78	5.17	16.17
No.10 RMBE (%)	0.31	15.16	−1.93	0.37	−1.53	−2.91	−3.69	−2.91	−2.09	8.28	25.00	1.79	−10.61
No.11 RRMSE (%)	12.38	11.62	32.81	12.41	9.96	16.25	13.84	16.60	19.34	9.12	22.49	6.65	24.07
No.11 RMBE (%)	−8.85	−10.37	−15.90	−8.85	−1.60	14.25	11.24	14.18	17.80	4.14	−5.55	3.10	−21.27
No.12 RRMSE (%)	6.34	29.36	26.85	6.56	6.18	5.35	5.44	6.11	6.01	15.39	94.29	10.82	19.70
No.12 RMBE (%)	2.65	28.39	13.37	2.73	0.88	0.75	−0.67	1.92	2.38	13.98	76.81	8.73	−14.75
No.13 RRMSE (%)	6.72	7.76	26.47	6.68	5.54	4.78	5.29	4.71	4.41	4.22	3.44	6.27	13.80
No.13 RMBE (%)	−5.97	−2.72	−17.59	−5.93	−4.66	−2.65	−3.56	−3.11	−1.66	1.84	1.16	−4.12	−13.04
No.14 RRMSE (%)	20.82	58.96	58.28	20.83	10.17	17.09	18.45	16.05	15.97	27.26	29.38	20.12	19.68
No.14 RMBE (%)	−20.46	−58.50	−52.82	−20.47	−8.96	−10.35	−11.85	−9.57	−8.94	−26.00	22.55	−19.28	−19.16
No.15 RRMSE (%)	13.36	60.64	51.10	13.35	9.81	22.72	21.70	21.91	23.88	16.91	70.55	4.19	19.21
No.15 RMBE (%)	−11.50	−60.57	−46.01	−11.49	4.89	21.30	20.31	19.88	22.42	−15.77	69.72	−1.23	−17.26
No.16 RRMSE (%)	7.05	28.14	30.19	7.03	6.11	10.30	9.60	11.50	11.27	8.29	39.81	4.19	13.46
No.16 RMBE (%)	4.29	27.97	8.29	4.26	−1.90	−9.08	−8.32	−10.16	−10.11	5.29	36.06	1.97	−9.74
No.17 RRMSE (%)	10.14	32.76	26.25	10.24	9.21	10.16	8.55	11.50	12.69	21.37	115.70	18.23	19.90
No.17 RMBE (%)	6.62	29.81	17.16	6.71	5.28	6.45	4.21	8.24	9.12	19.56	92.03	14.38	−9.92
No.18 RRMSE (%)	4.32	29.09	17.99	4.39	3.38	4.26	2.85	5.51	6.52	15.92	95.22	12.49	19.17
No.18 RMBE (%)	3.65	26.60	12.81	3.73	2.15	2.52	0.74	3.91	4.59	15.39	77.14	9.98	−11.48
No.19 RRMSE (%)	7.56	37.32	35.47	7.73	13.40	46.53	47.32	45.28	46.15	23.00	88.32	17.69	20.37
No.19 RMBE (%)	3.61	−37.09	−26.28	3.71	10.95	44.58	45.68	43.87	43.90	−22.59	84.76	13.20	−18.02
No.20 RRMSE (%)	4.99	23.94	18.43	5.08	7.32	9.57	10.33	9.16	8.94	6.59	117.87	6.71	23.45
No.20 RMBE (%)	−2.35	22.32	8.96	−2.28	−5.76	−8.71	−9.53	−8.20	−7.89	4.69	93.77	1.90	−19.32
No.21 RRMSE (%)	3.87	33.49	26.83	3.94	5.97	9.16	9.83	9.04	8.70	7.31	167.20	7.64	25.18
No.21 RMBE (%)	0.59	33.11	16.88	0.58	−4.06	−8.50	−9.16	−8.06	−8.05	5.54	164.43	6.82	−24.52

**Table 8.** Summary of model performance with general equations.

Station \ Model	No.1	No.2	No.3	No.4	No.5	No.6	No.7	No.8	No.9	No.10	No.11	No.12	No.13	
Stations No.1–8	RRMSE (%)	9.94	24.13	36.94	9.95	9.63	9.51	10.02	9.50	9.24	19.53	26.61	10.43	13.99
	NRMSE (%)	10.63	25.53	44.91	10.62	11.41	10.81	11.35	10.77	10.53	25.00	26.96	11.59	18.80
	RMBE (%)	0.96	2.33	−13.78	0.97	−0.89	−2.04	−2.85	−2.02	−1.33	−3.73	15.34	0.27	−3.84
	NMBE (%)	−0.37	1.43	−24.96	−0.38	−2.48	−2.88	−3.68	−3.08	−2.16	−5.89	13.13	0.06	−4.47
	NSE	0.9372	0.6375	−0.1221	0.9373	0.9276	0.9350	0.9283	0.9355	0.9383	0.6523	0.5958	0.9252	0.8034
	R <sup>2</sup>	0.9374	0.7198	0.2322	0.9375	0.9328	0.9397	0.9360	0.9413	0.9409	0.6878	0.7517	0.9290	0.8254
	$\sigma_{sn}$	0.9582	1.1333	0.5699	0.9581	0.9234	0.9602	0.9565	0.9467	0.9647	0.9565	1.1118	1.0254	1.0126
	E <sub>n</sub> ' (%)	25.05	60.11	88.07	25.02	26.27	24.57	25.32	24.34	24.31	57.31	55.52	27.35	43.06
All stations	RRMSE (%)	10.52	34.11	35.99	10.55	8.81	14.98	15.06	14.75	15.23	17.77	68.97	10.99	18.28
	NRMSE (%)	12.33	39.26	43.20	12.28	9.54	16.94	17.02	16.14	17.30	21.28	93.65	12.97	24.79
	RMBE (%)	−1.82	−1.94	−11.79	−1.79	−0.65	2.21	1.30	2.28	3.17	−2.00	44.05	1.46	−11.66
	NMBE (%)	−3.39	−1.47	−21.11	−3.58	−2.46	1.67	0.59	1.44	2.83	−3.20	50.79	1.97	−14.89
	NSE	0.9250	0.2400	0.0800	0.9257	0.9551	0.8586	0.8571	0.8716	0.8525	0.7766	−3.3238	0.9171	0.6970
	R <sup>2</sup>	0.9316	0.5695	0.3459	0.9316	0.9614	0.8764	0.8707	0.8838	0.8782	0.7989	0.5948	0.9322	0.8221
	$\sigma_{sn}$	0.9354	1.3277	0.8033	0.9347	0.9227	1.0642	1.0488	1.0459	1.0844	1.0251	2.3981	1.0804	0.7810
	E <sub>n</sub> ' (%)	26.32	87.12	83.69	26.33	20.47	37.42	37.78	35.69	37.89	46.72	174.70	28.46	44.01

Table 8 and Figure 10a indicate that for stations No.1–8 the best results are obtained by the one-parameter models No.1, No.4 and No.5, and by the two-parameter models No.6–9, with indicators similar to and slightly better than those of model No.12. However, Table 7 shows very high RRMSE values for models No.6–9 at station No.19. Comparisons between models No.5 and No.10, as well as models No.8 and No.11, with the same variables but different number of parameters, are examples of improvement with increasing degrees of freedom.

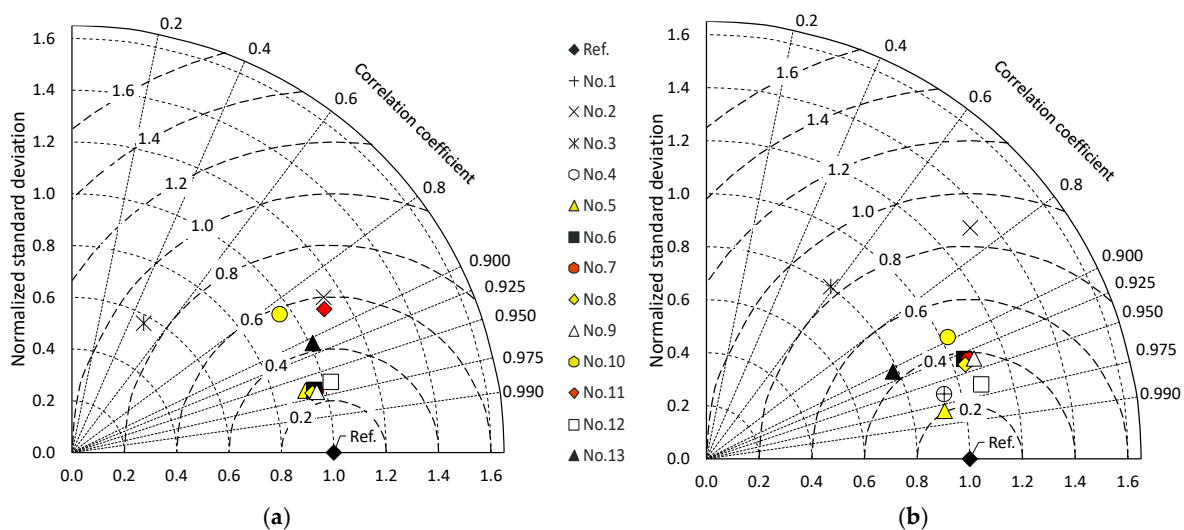


**Figure 10.** Comparison of model performance with general equations: (a) Stations No.1–8; (b) all stations.

For the set of 21 stations, Table 8 shows that model No.5 obtains the best values for each statistical indicator, as Figure 10b confirms. Furthermore, Table 7 shows that the maximum local values of RRMSE are lower for model No.5 (13.40% at station No.19) than for the other models (e.g., 20.82% and 20.83%, respectively for models No.1 and No.4 at station No.14).

#### 4. Solar Map of Asturias

Model No.5 was developed more than a decade ago as a starting point for the edition of the first SMA, using data up to 2005 and different periods due to lack of measurements at some stations [17]. As a consequence of the results obtained in the previous section, this model has been selected to update the SMA in the framework of the project RehabilitaGeoSol [39], using data from stations No.1–8 during the same period, i.e., 2003–2016. In addition, the model has, recently, been found to be consistent with recommendations to improve the predictive capability of GSR models in regions with sparse radiometric stations [40], namely (a) selecting appropriate variables to represent the climate of the region; (b) using ratios of variables as model inputs to improve the generality of the model; and (c) considering that a higher R-squared value is necessary for the significance of a model at a given probability level, if the degrees of freedom are reduced by using a larger number of constant coefficients.

The Digital Elevation Model of the Principality of Asturias, and the temperature data measured at 87 thermometric stations of the AEMET network, were used for the update. The monthly GSR values calculated using Equations (5) and (23) were processed using ArcGIS software [41], for graphical representation. To facilitate comparisons with state-wide classifications [42], irradiation maps were constructed with GSR isolines at 0.4 kWh/(m<sup>2</sup>·day) intervals. Figure 11 shows the annual average GSR map on a horizontal surface, while the monthly maps can be found in Appendix A.

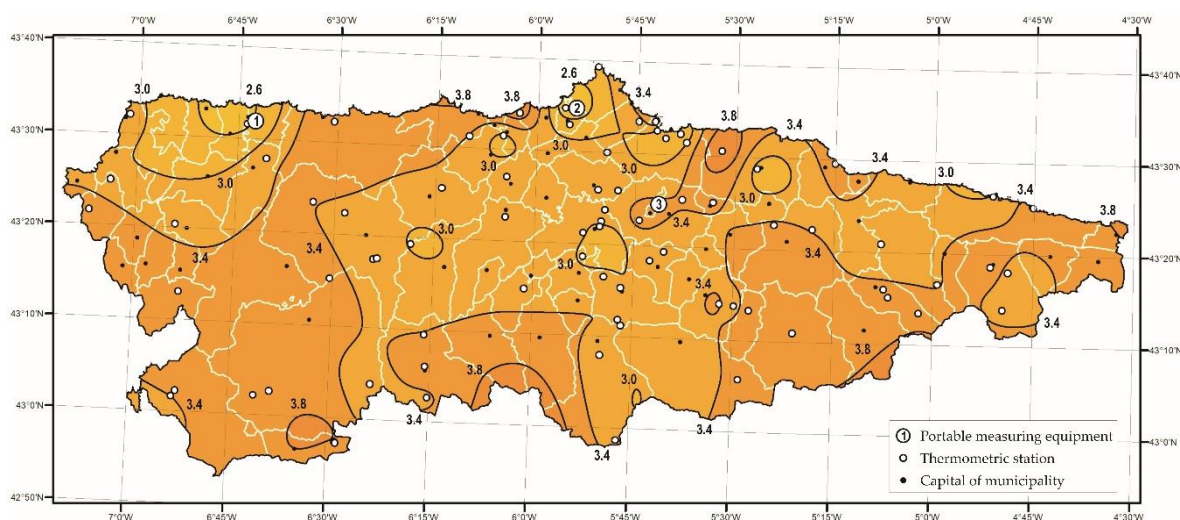


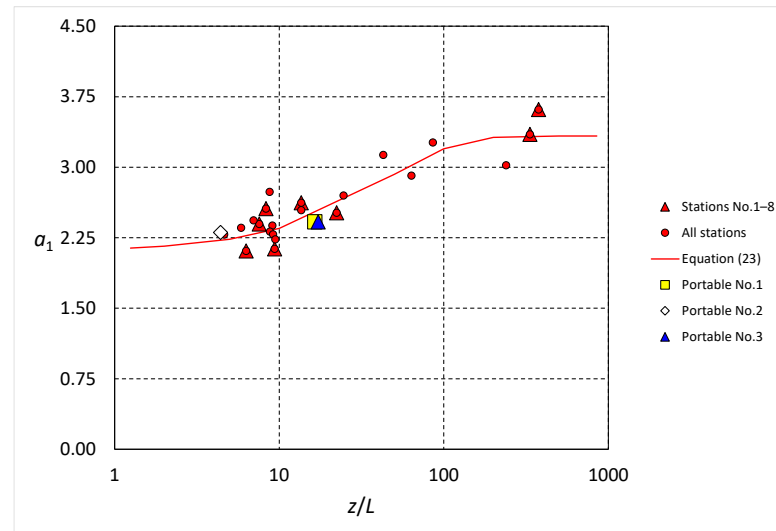
**Figure 11.** Annual averages of global solar irradiation on horizontal surfaces in Asturias (kWh/m<sup>2</sup>·day).

As a first evaluation of the results, GSR estimates for the western part of the region, where radiometric stations are not available, were compared with the solar radiation atlas published for the bordering region, based on Meteosat satellite images for the period 1985–2008 [43], showing an acceptable agreement despite methodological differences.

As further corroboration, measurements were performed using three portable units equipped with Kipp & Zonen CMP-11 pyranometers, the first two of which were located in coastal areas with low annual GSR averages that might be caused by the surrounding industrial activity. Table 9 and Figure 11 indicate the location coordinates and the values of the coefficient  $a_1$  deduced from measurements obtained during 2010 and 2011. As shown in Figure 12, the results are in agreement with the predictions of Equation (23).

**Table 9.** Location of portable weather stations and measurement results.

No.	Locality	$\varphi$ (°N)	$\lambda$ (°W)	$z$	$L$	$z/L$	$a_1$
1	Navia	43.522	6.725	65	3.95	16.46	2.481
2	Avilés	43.555	5.893	24	5.46	4.40	2.308
3	San Pedro de Anes	43.430	5.700	218	12.65	17.23	2.420

**Figure 12.** Validation of the GSR model using portable equipment.

Since, at least in regions with moderate monthly variation of relative humidity, the energy demand is determined by air temperature and GSR maps, it is justified that the described procedure has been used to identify climatic zones in regions with varied orography and proximity to the sea [44–46].

To limit energy demand, the Spanish Technical Building Code (TBC) [42] prescribes a minimum contribution for solar water heating (SWH) and a maximum transmissivity of enclosures depending on the climate zone. For SWH contribution calculations, the TBC establishes five climate zones, based on the annual average GSR, at  $0.4 \text{ kWh}/(\text{m}^2 \cdot \text{day})$  intervals. Most of Asturias is in climate zone I, defined by  $\bar{H} < 3.8 \text{ kWh}/(\text{m}^2 \cdot \text{day})$ , but according to Figure 11, the solar irradiation over about half of the region is  $\bar{H} < 3.0 \text{ kWh}/(\text{m}^2 \cdot \text{day})$ , so the TBC requirement for SWH is demanding in this area. For transmissivity calculations, 12 climate zones are defined on the basis of the climate severity index (CSI), which is dimensionless and depends on the degree-days ( $DD$ ) and GSR. The simplified calculation procedure makes it possible to select the climate zone of a locality on the basis of altitude, but may lead to questionable results in coastal areas of varying orography. Figure 13 shows the three climate zones calculated using ArcGIS, on a  $25 \times 25 \text{ m}$  grid, for the average altitude of each postal district in Asturias. The thicker dividing lines indicate municipality boundaries and the thinner ones delimit postal districts. Although Asturias is the province with the longest coastline in Spain, only 9.7% of the region would be in climate zone C1, which seems to underestimate the thermal regulation of the sea. A more advanced option allows estimating  $DD$  and GSR values at a location without records by interpolation of data from other locations, and calculating the CSI that determines the climate zone by the following equation:

$$CSI = a_1 DD + a_2 DD^2 + a_3 (S/S_0) + a_4 (S/S_0)^2 + a_5 \quad (43)$$



**Figure 13.** Climatic zones in Asturias calculated for the average altitude of each postcode district.

This interpolation procedure is well contrasted and takes into account the differences in latitude, altitude and distance to the sea [47–49], however, to take advantage of the breadth of the network of thermometric stations, it could be interesting to replace the last three summands of Equation (43), i.e., the model of Ögelman et al. [50], by the model based on Equations (5) and (23). Additionally, improvements can be expected by normalising  $DD$  to obtain a dimensionally homogeneous equation and, thus, avoid the influence of implicit variables in the coefficients  $a_1$  and  $a_2$ .

## 5. Conclusions

The trade-off between exactitude, complexity and generality has been analysed for 13 temperature-based GSR models, using data from 21 meteorological stations along the northern Spanish coastal area.

Using site-calibrated coefficients, accuracy can improve with model complexity, without remarkable advantages, due to the use of dimensionally homogeneous equations. Most models have high accuracy and none improve on the others at any location.

The influence of geographical variables on the local coefficients has been analysed, using the  $z/L$  ratio as a variable, in order to avoid the influence of variables implicit in the coefficients of non-dimensionally homogeneous equations. The coefficients obtained for each location, by means of general equations, are, generally, more dispersed for models with a greater number of parameters. The homogeneous one-parameter model No.5 obtained the best results for each of the statistical quality indicators in the set of 21 stations, which suggests recommending dimensionally homogeneous models with the highest number of degrees of freedom, for estimations in areas with sparse GSR data.

This model has been used to update the Solar Map of Asturias using GIS techniques and data measured during the same time period at 87 thermometric stations. The procedure allows the definition of monthly average GSR isolines in regions with sparse radiometric data, however, future work is needed to study the performance of the model under different climatic conditions and latitudes.

**Author Contributions:** Conceptualization, J.-I.P.; Data curation, D.G. and R.S.; Formal analysis, D.G.; Funding acquisition, J.-I.P.; Methodology, J.-I.P.; Supervision, J.-I.P.; Writing—original draft, J.-I.P.; Writing—review & editing, D.G. All authors have read and agreed to the published version of the manuscript.

**Funding:** This research has been developed in the framework of the multidisciplinary R&D project ‘Energy Efficiency through Rehabilitation, the Sun and Geothermal Energy in Asturias’ (RehabilitaGeoSol, RTC-2016-5004-3), supported by the Spanish Ministry of Science and Innovation and co-financed by the European Regional Development Funds (ERDF).

**Institutional Review Board Statement:** Not applicable.

**Informed Consent Statement:** Not applicable.

**Data Availability Statement:** Not applicable.

**Conflicts of Interest:** The authors declare no conflict of interest. The funders had no role in the design of the study; in the collection, analyses, or interpretation of data; in the writing of the manuscript, or in the decision to publish the results.

## Nomenclature

$a_i$	Empirical parameter
$DD$	Degree-days ( $^{\circ}\text{C} \cdot \text{day}$ )
$E'$	Centred pattern RMSE ( $\text{kWh}/\text{m}^2$ ) = $\sqrt{\sum_{i=1}^n [(s_i - \bar{s}_i)^2 - (o_i - \bar{o}_i)^2] / n}$
$E'_n$	Normalised centred pattern RMSE = $E' / \sigma_o$
$H$	Global solar irradiation on horizontal surface ( $\text{kWh}/\text{m}^2$ )
$H_0$	Extraterrestrial global solar irradiation on horizontal surface ( $\text{kWh}/\text{m}^2$ )
KGCC	Köppen-Geiger climate classification
$L$	Distance to the sea (m)
MBE	Mean bias error ( $\text{kWh}/\text{m}^2$ ) = $\sum_{i=1}^n (s_i - o_i) / n$
NMBE	Normalised mean bias error = $(\sum_{i=1}^n (s_i - o_i) / n) / \bar{o}_i$
NRMSE	Normalised root mean square error = $\left( \sqrt{\sum_{i=1}^n (s_i - o_i)^2 / n} \right) / \bar{o}_i$
NSE	Nash-Sutcliffe model efficiency = $1 - \sum_{i=1}^n (s_i - o_i)^2 / \sum_{i=1}^n (o_i - \bar{o}_i)^2$
$o_i$	Observed value
$R^2$	Coefficient of determination = $\left[ \frac{\sum_{i=1}^n (s_i - \bar{s}_i)(o_i - \bar{o}_i) / \sqrt{\sum_{i=1}^n (s_i - \bar{s}_i)^2 \sum_{i=1}^n (o_i - \bar{o}_i)^2}} \right]^2$
RMSE	Root mean square error ( $\text{kWh}/\text{m}^2$ ) = $\sqrt{\sum_{i=1}^n (s_i - o_i)^2 / n}$
RMBE	Relative mean bias error = $\sum_{i=1}^n ((s_i - o_i) / o_i) / n$
RRMSE	Relative root mean square error = $\sqrt{\sum_{i=1}^n ((s_i - o_i) / o_i)^2 / n}$
$S_0$	Maximum theoretical duration of sunshine (h)
$S$	Actual duration of sunshine (h)
$s_i$	Simulated value
$T_m$	Mean air temperature (K)
$T_{\max}$	Maximum air temperature (K)
$T_{\min}$	Minimum air temperature (K)
$z$	Elevation above sea level (m)
$\Delta T$	Temperature difference (K) = $T_{\max} - T_{\min}$
$\varphi$	Latitude (rad)
$\lambda$	Longitude (rad)
$\sigma_o$	Standard deviation of experimental solar irradiation ( $\text{kWh}/\text{m}^2$ ) = $\sqrt{(\sum_{i=1}^n (o_i - \bar{o}_i)^2) / n}$
$\sigma_s$	Standard deviation of simulated solar irradiation ( $\text{kWh}/\text{m}^2$ ) = $\sqrt{(\sum_{i=1}^n (s_i - \bar{s}_i)^2) / n}$
$\sigma_{sn}$	Normalised standard deviation = $\sigma_s / \sigma_o$

### Appendix A

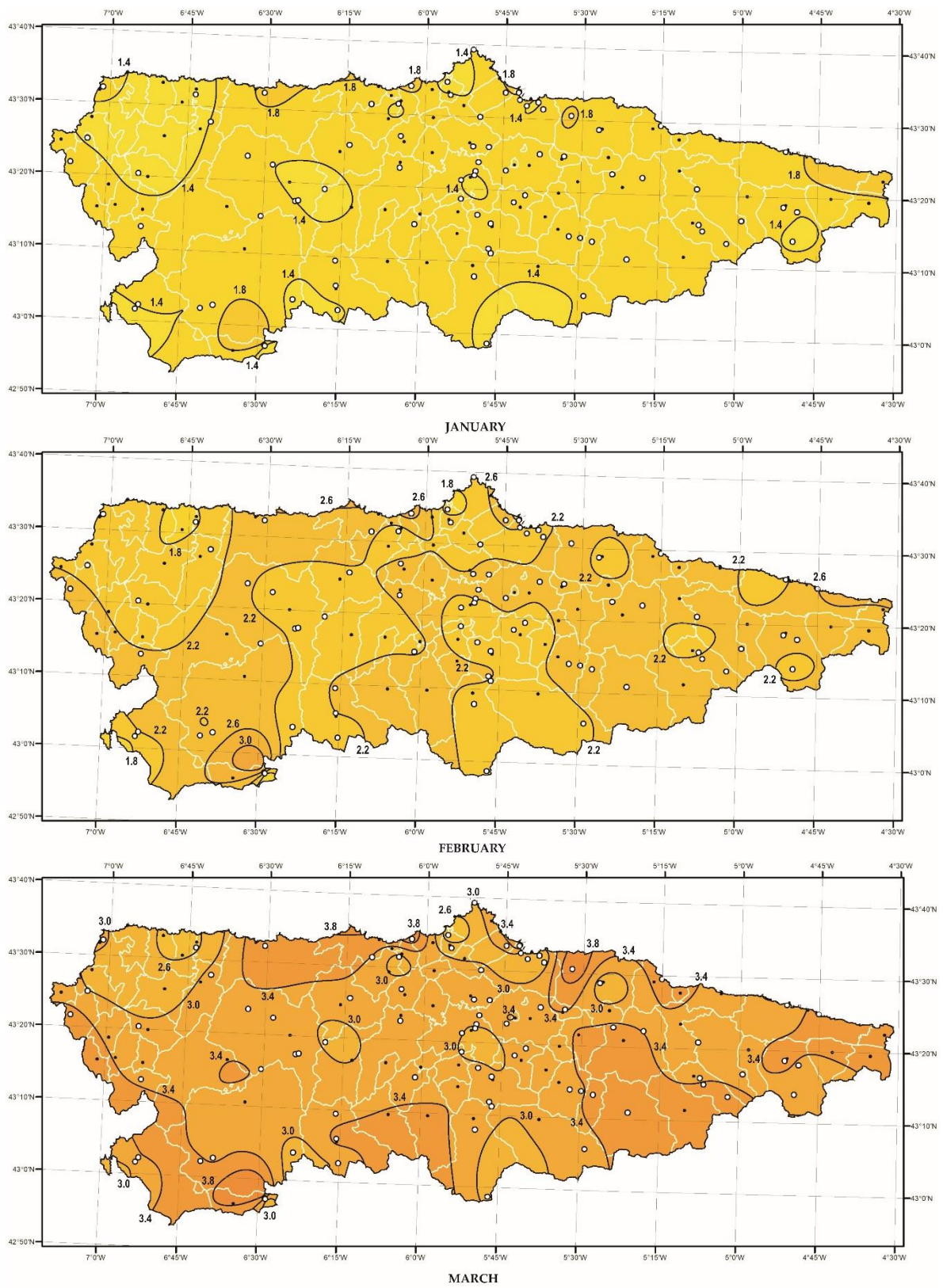


Figure A1. Cont.

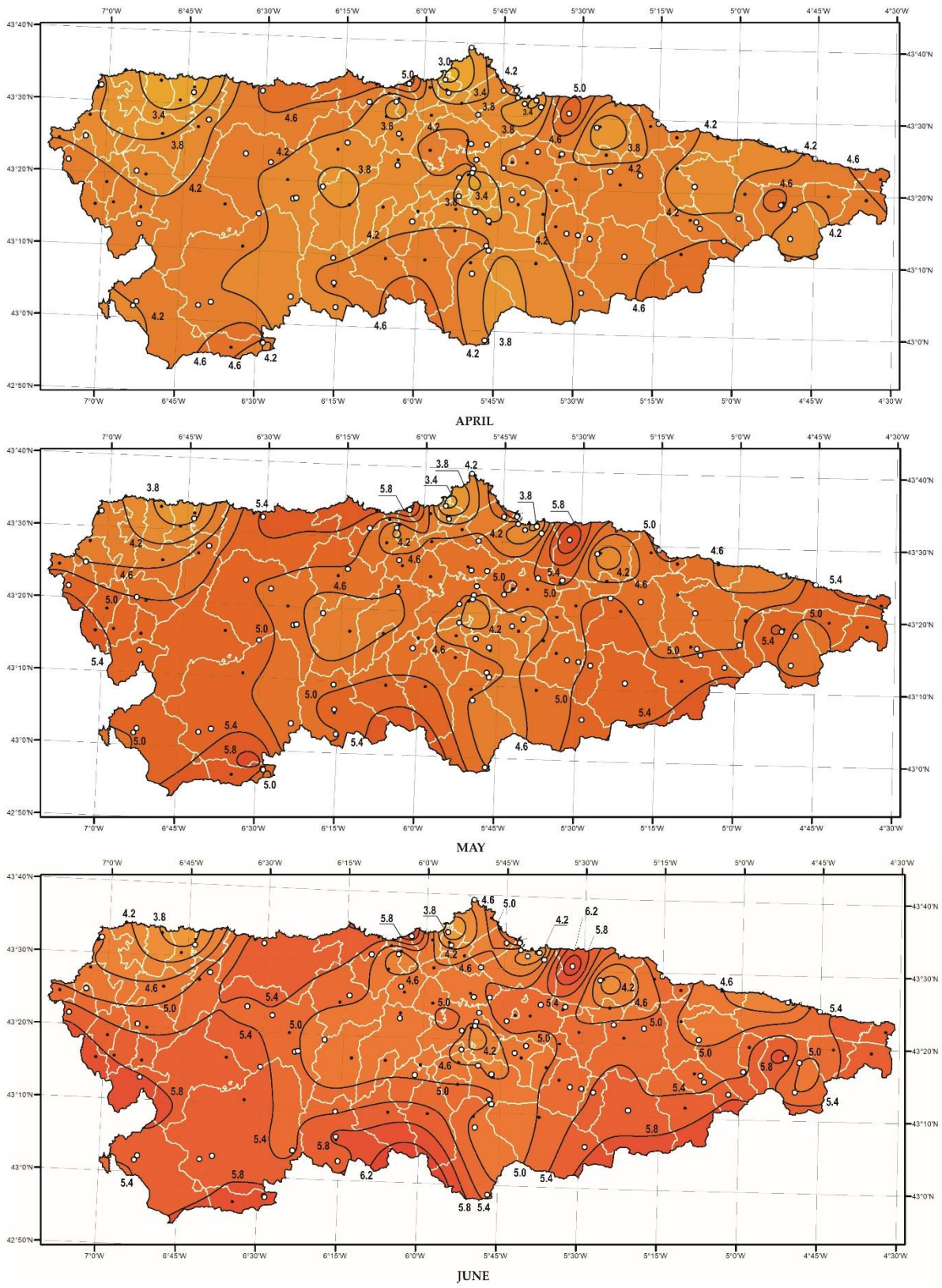


Figure A1. Cont.

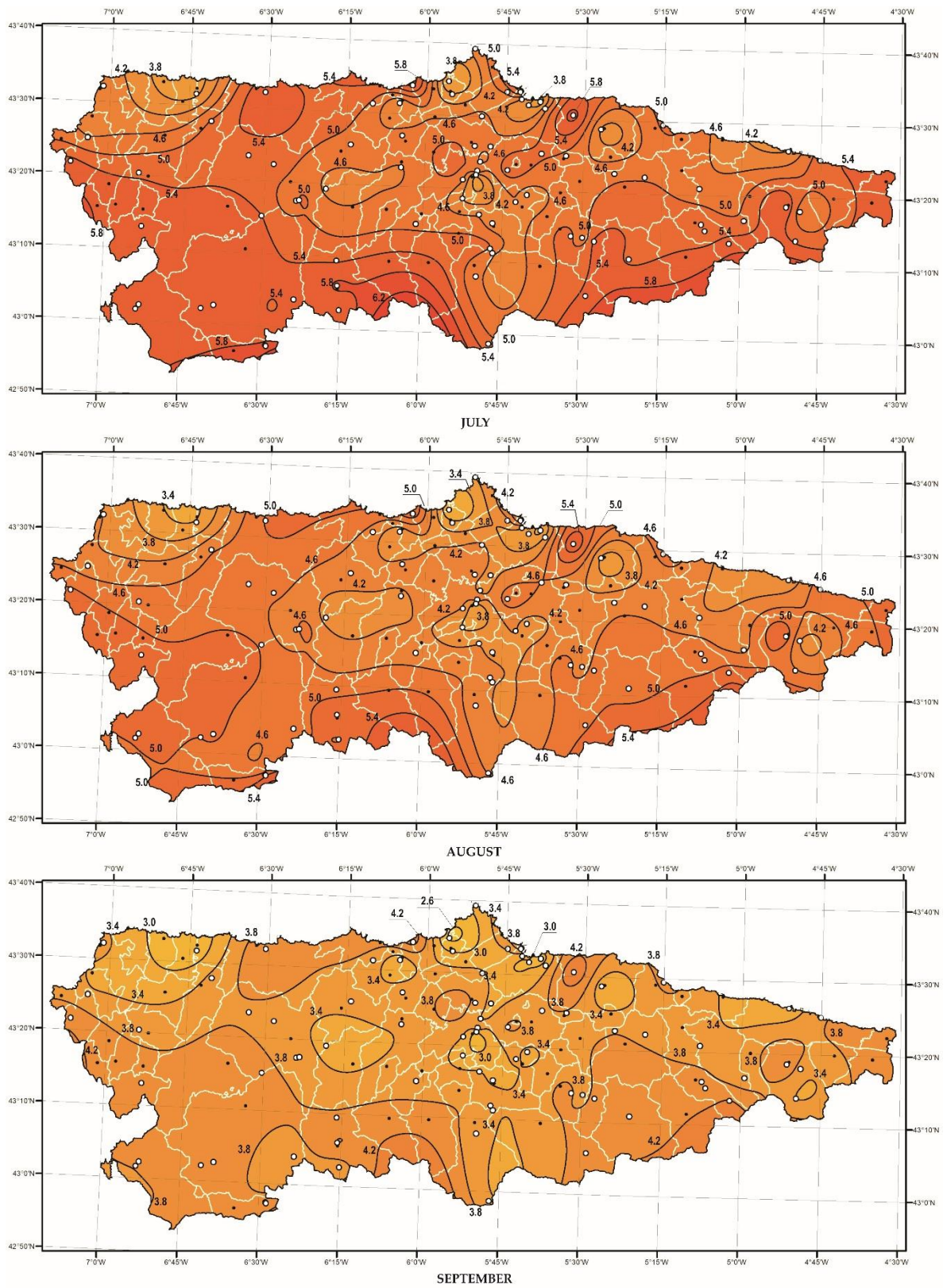
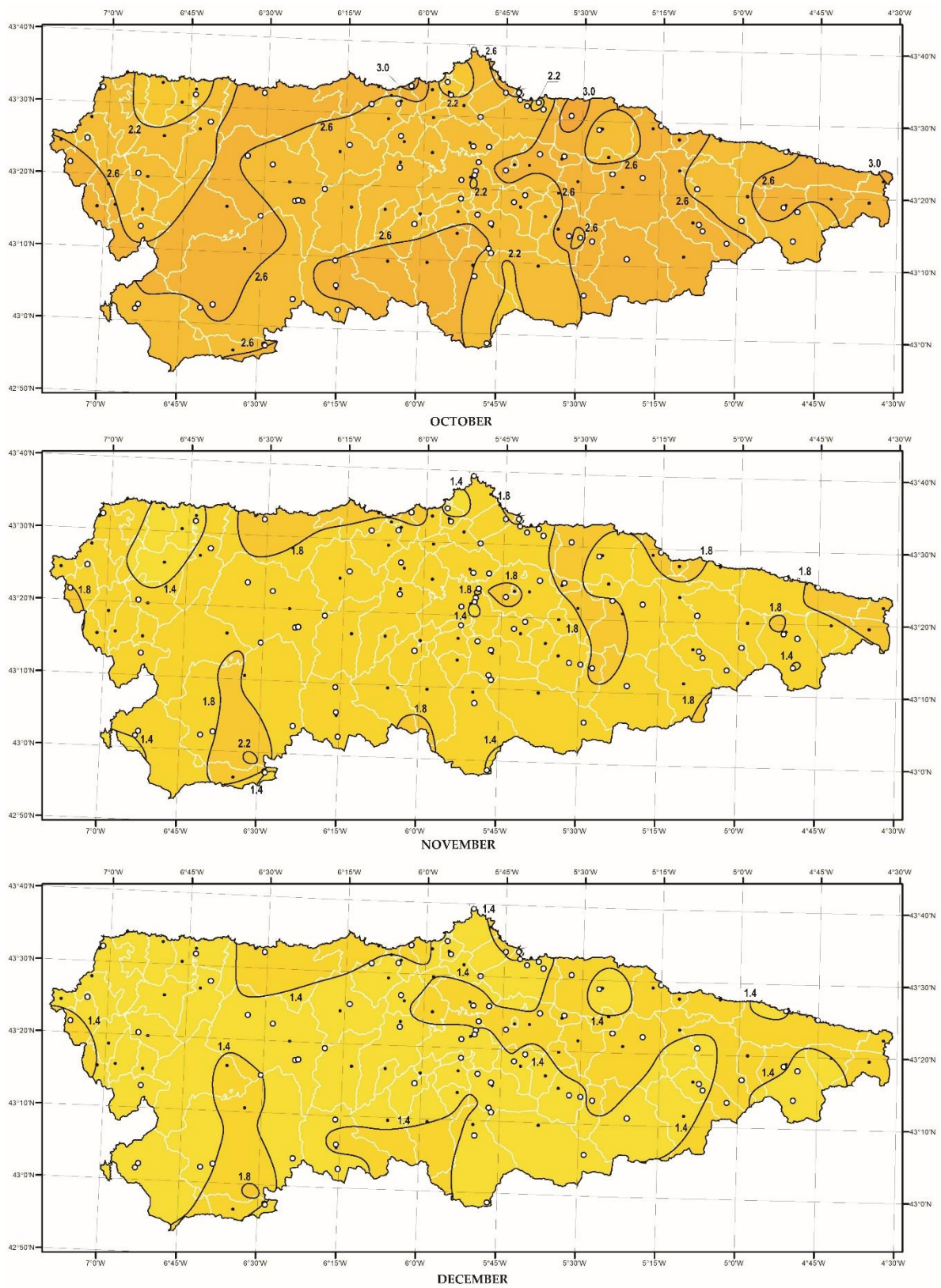


Figure A1. Cont.



**Figure A1.** Monthly averages of global solar irradiation on horizontal surfaces in Asturias (kWh/m<sup>2</sup>·day).

## References

- Behar, O.; Khellaf, A.; Mohammedi, K. Comparison of solar radiation models and their validation under Algerian climate—The case of direct irradiance. *Energy Convers. Manag.* **2015**, *98*, 236–251. [\[CrossRef\]](#)
- Muneer, T.; Younes, S.; Munawwar, S. Discourses on solar radiation modeling. *Renew. Sustain. Energy Rev.* **2007**, *11*, 551–602. [\[CrossRef\]](#)
- Thornton, P.E.; Running, S.W. An improved algorithm for estimating incident daily solar radiation from measurements of temperature, humidity, and precipitation. *Agric. Forest Meteorol.* **1999**, *93*, 211–228. [\[CrossRef\]](#)
- Zang, H.X.; Xu, Q.S.; Bian, H.H. Generation of typical solar radiation data for different climates of China. *Energy* **2012**, *38*, 236–248. [\[CrossRef\]](#)
- Antoñanzas, F.; Sanz, A.; Martínez-de-Pisón, F.J.; Perpiñán, O. Evaluation and improvement of empirical models of global solar irradiation: Case study northern Spain. *Renew. Energy* **2013**, *60*, 604–614. [\[CrossRef\]](#)
- Chen, J.L.; He, L.; Yang, H.; Ma, M.; Chen, Q.; Wu, S.J.; Xiao, Z.L. Empirical models for estimating monthly global solar radiation: A most comprehensive review and comparative case study in China. *Renew. Sustain. Energy Rev.* **2019**, *108*, 91–111. [\[CrossRef\]](#)
- Abraha, M.G.; Savage, M.J. Comparison of estimates of daily solar radiation from air temperature range for application in crop simulations. *Agr. Forest Meteorol.* **2008**, *148*, 401–416. [\[CrossRef\]](#)
- Myers, D.R. Solar radiation modeling and measurements for renewable energy applications: Data and model quality. *Energy* **2005**, *30*, 1517–1531. [\[CrossRef\]](#)
- Prieto, J.I.; García, D. Global solar radiation models: A critical review from the point of view of homogeneity and case study. *Renew. Sustain. Energy Rev.* **2022**, *155*, 111856. [\[CrossRef\]](#)
- Elagib, N.; Mansell, M.G. New approaches for estimating global solar radiation across Sudan. *Energy Convers. Manag.* **2000**, *41*, 419–434. [\[CrossRef\]](#)
- Jin, Z.; Yezhen, W.; Gang, Y. General formula for estimation of monthly average daily global solar radiation in China. *Energy Convers. Manag.* **2005**, *46*, 57–268. [\[CrossRef\]](#)
- Chen, R.; Kang, E.; Ji, X.; Yang, J.; Zhang, Z. Trends of the global radiation and sunshine hours in 1961–1998 and their relationships in China. *Energy Convers. Manag.* **2006**, *47*, 2859–2866. [\[CrossRef\]](#)
- Robaa, S.M. Validation of the existing models for estimating global solar radiation over Egypt. *Energy Convers. Manag.* **2009**, *50*, 184–193. [\[CrossRef\]](#)
- Paulescu, M.; Stefu, N.; Calinoiu, D.; Paulescu, E.; Pop, N.; Boata, R.; Mares, O. Ångström–Prescott equation: Physical basis, empirical models and sensitivity analysis. *Renew. Sustain. Energy Rev.* **2016**, *62*, 495–506. [\[CrossRef\]](#)
- Annandale, J.G.; Jovanovic, N.Z.; Benadé, N.; Allen, R.G. Software for missing data error analysis of Penman–Monteith reference evapotranspiration. *Irrig. Sci.* **2002**, *21*, 57–67.
- Prieto, J.I.; Martínez-García, J.C.; García, D. Correlation between global solar irradiation and air temperature in Asturias, Spain. *Sol. Energy* **2009**, *83*, 1076–1085. [\[CrossRef\]](#)
- Prieto, J.I.; Martínez, J.C.; García, D.; Santoro, R.; Rodríguez, A. *Solar Map of Asturias*; Consorcio de Empresas ARFRISOL: Gijón, Spain, 2009; p. 197. (In Spanish)
- Hargreaves, G.H.; Samani, Z.A. Estimating potential evapotranspiration. *J. Irrig. Drain. Eng. ASCE* **1982**, *108*, 225–230. [\[CrossRef\]](#)
- Hargreaves, G.H. *Simplified Coefficients for Estimating Monthly Solar Radiation in North America and Europe*; Dept. Paper, Dept. Biol. and Irrig. Engrg.; Utah State University: Logan, UT, USA, 1994.
- Meza, F.; Varas, E. Estimation of mean monthly solar global radiation as a function of temperature. *Agric. Forest Meteorol.* **2000**, *100*, 231–241. [\[CrossRef\]](#)
- Bristow, K.L.; Campbell, G.S. On the relationship between incoming solar radiation and daily maximum and minimum temperature. *Agr. Forest Meteorol.* **1984**, *31*, 159–166. [\[CrossRef\]](#)
- Weiss, A.; Hays, C.J.; Hu, Q.; Easterling, W.E. Incorporating bias error in calculating solar irradiance: Implications for crop yield simulations. *Agron. J.* **2001**, *93*, 1321–1326. [\[CrossRef\]](#)
- Goodin, D.G.; Hutchinson, J.M.S.; Vanderlip, R.L.; Knapp, M.C. Estimating solar irradiance for crop modeling using daily air temperature data. *Agron. J.* **1999**, *91*, 845–851. [\[CrossRef\]](#)
- Bandyopadhyay, A.; Bhadra, A.; Raghuvanshi, N.S.; Singh, R. Estimation of monthly solar radiation from measured air temperature extremes. *Agric. Forest Meteorol.* **2008**, *148*, 1707–1718. [\[CrossRef\]](#)
- Allen, R.G. *Evaluation of Procedures for Estimating Mean Monthly Solar Radiation from Air Temperature*; Technical Report; United Nations Food and Agric. Org. (FAO): Rome, Italy, 1995.
- Hargreaves, G.L.; Hargreaves, G.H.; Riley, J.P. Irrigation water requirements for Senegal River Basin. *J. Irrig. Drain. Eng.* **1985**, *111*, 265–275. [\[CrossRef\]](#)
- Supit, I.; van Kappel, R.R. A simple method to estimate global radiation. *Sol. Energy* **1998**, *63*, 147–160. [\[CrossRef\]](#)
- Hunt, L.A.; Kucharb, L.; Swanton, C.J. Estimation of solar radiation for use in crop modeling. *Agric. Forest Meteorol.* **1998**, *91*, 293–300. [\[CrossRef\]](#)
- Chen, R.; Ersi, K.; Yang, J.; Lu, S.; Zhao, W. Validation of five global radiation models with measured daily data in China. *Energy Convers. Manag.* **2004**, *45*, 1759–1769. [\[CrossRef\]](#)
- Pandey, C.K.; Katiyar, A.K. Temperature base correlation for the estimation of global solar radiation on horizontal surface. *Int. J. Energy Environ.* **2010**, *1*, 737–744.

31. Chen, J.L.; Li, G.S. Estimation of monthly average daily solar radiation from measured meteorological data in Yangtze River Basin in China. *Int. J. Climatol.* **2013**, *33*, 487–498. [CrossRef]
32. Richardson, C.W. Weather simulation for crop management models. *Trans. ASAE* **1985**, *28*, 1602–1606. [CrossRef]
33. Li, M.; Liu, H.; Guo, P.; Wu, W. Estimation of daily solar radiation from routinely observed meteorological data in Chongqing, China. *Energy Convers. Manag.* **2010**, *51*, 2575–2579. [CrossRef]
34. Hassan, G.E.; Youssef, M.E.; Mohamed, Z.E.; Ali, M.A.; Hanafy, A.A. New Temperature-based Models for Predicting Global Solar Radiation. *Appl. Energy* **2016**, *179*, 437–450. [CrossRef]
35. Chazarra, A.; Flórez, E.; Peraza, B.; Tohá, T.; Lorenzo, B.; Criado, E.; Moreno, J.V.; Romero, R.; Botey, R. *Mapas Climáticos de España (1981–2010) y ETo (1996–2016)*; AEMET: Madrid, Spain, 2018; (In Spanish). [CrossRef]
36. Lewis, C. *International and Business Forecasting Methods*; Butterworths: London, UK, 1982; p. 143.
37. Gueymard, C.A. A review of validation methodologies and statistical performance indicators for modeled solar radiation data: Towards a better bankability of solar projects. *Renew. Sustain. Energy Rev.* **2014**, *39*, 1024–1034. [CrossRef]
38. Taylor, K.E. Summarizing multiple aspects of model performance in a single diagram. *J. Geophys. Res.* **2001**, *106*, 7183–7192. [CrossRef]
39. Soutullo, S.; Giancola, E.; Sánchez, M.N.; Ferrer, J.A.; García, D.; Suárez, M.J.; Prieto, J.I.; Antuña-Yudego, E.; Carús, J.L.; Fernández, M.A.; et al. Methodology for Quantifying the Energy Saving Potentials Combining Building Retrofitting, Solar Thermal Energy and Geothermal Resources. *Energy* **2020**, *13*, 5970. [CrossRef]
40. Mirzabe, A.H.; Hajiahmad, A.; Keyhani, A.; Mirzaei, N. Approximation of daily solar radiation: A comprehensive review on employing of regression models. *Renew. Energy Focus* **2022**, *41*, 143–159. [CrossRef]
41. ArcGIS Desktop 9.3 Service Pack 1, ESRI. 2008.
42. Royal Decree 314/2006, Approved 17th May, in which Technical Building Code for Spain is Approved. Available online: <https://www.global-regulation.com/translation/spain/1446654/royal-decree-314-2006%252c-of-march-17%252c-which-approves-the-technical-building-code.html> (accessed on 11 May 2022).
43. Vázquez, M.; Santos, J.M.; Prado, M.T.; Vázquez, D.; Rodrigues, F.M. *Atlas de Radiación Solar de Galicia*; Universidad de Vigo: Vigo, Spain, 2005. Available online: [https://www.meteogalicia.gal/datosred/infoweb/meteo/docs/publicacions/libros/Atlas\\_Radiacion\\_Solar\\_Galicia.pdf](https://www.meteogalicia.gal/datosred/infoweb/meteo/docs/publicacions/libros/Atlas_Radiacion_Solar_Galicia.pdf) (accessed on 11 May 2022).
44. Attia, S.; Lacombe, T.; Rakotondramiarana, H.T.; Garde, F.; Roshan, G.R. Analysis tool for bioclimatic design strategies in hot humid climates. *Sustain. Cities Soc.* **2019**, *45*, 8–24. [CrossRef]
45. Praene, J.P.; Malet-Damour, B.; Radanielina, M.H.; Fontaine, L.; Rivière, G. GIS-based approach to identify climatic zoning: A hierarchical clustering on principal component analysis. *Build. Environ.* **2019**, *164*, 106330. [CrossRef]
46. Dailidė, R.; Povilanskas, R.; Méndez, J.A.; Simanavičiūtė, G. A new approach to local climate identification in the Baltic Sea’s coastal area. *Baltica* **2019**, *32*, 210–218. [CrossRef]
47. Sánchez, F.J.; Salmerón, J.M.; Domínguez, S.A. A new methodology towards determining building performance under modified outdoor conditions. *Build. Environ.* **2006**, *41*, 1231–1238.
48. Sánchez, F.J.; Domínguez, S.A.; Molina, J.M.; González, R. Climatic zoning and its application to Spanish building energy performance regulations. *Energy Build.* **2008**, *40*, 1984–1990.
49. Salmerón, J.M.; Álvarez, S.; Molina, J.L.; Ruiz, A.; Sánchez, F.J. Tightening the energy consumptions of buildings depending on their typology and on Climate Severity Indexes. *Energy Build.* **2013**, *58*, 372–377. [CrossRef]
50. Ögelman, H.; Ecevit, A.; Tasemiroglu, E. A new method for estimating solar radiation from bright sunshine data. *Sol. Energy* **1984**, *33*, 619–625. [CrossRef]